

People's Democratic Republic of Algeria
الجمهورية الجزائرية الديمقراطية الشعبية
Ministry of Higher Education and Scientific Research
وزارة التعليم العالي والبحث العلمي
University ABOU BEKR BELKAID of TLEMCEM
جامعة أبو بكر بلقايد- تلمسان
Faculty of Nature and Life Sciences, and Earth and Universe Sciences
Department of Biology
كلية علوم الطبيعة والحياة، وعلوم الأرض والكون



Final Dissertation

Presented by
Koudache Yacine

In order to obtain
Master's Degree
In Applied Biochemistry

Theme

Phosphorylation prediction of astrocytic connexins

Presented on July 4, 2024 before the jury composed of:

Chairman	Pr BENARIBA Nabila	Professor	Abou Bekr Belkaid University
Supervisor	Dr BRIKCI NIGASSA Amal	MCB	Abou Bekr Belkaid University
Examiner	Dr BENMANSOUR Meriem	MCA	Abou Bekr Belkaid University

Academic year 2023/2024

DEDICATION

First and foremost, we thank Almighty Allah for his help and
guidance.

To my beloved family, the sources of my success.

To my friends for their endless love, prayers and support.

To everyone who helped me and the ones I love.

Acknowledgement

In the preamble of this dissertation, I wish to express my gratitude to Almighty Allah for granting me the patience and courage necessary during these long years of study.

This work would not have been possible without the help and guidance of Dr BRIKCI NIGASSA Amal, whom I warmly thank for the exceptional quality of her supervision, her patience, and her availability throughout the completion of this dissertation.

I would also like to profoundly thank Pr BENARIBA Nabila for the honor she bestows upon me by agreeing to chair this jury.

My sincere thanks also go to Dr BENMANSOUR Meriem for agreeing to examine and discuss this work. I want to extend my most heartfelt thanks to all my professors for their exceptional efforts, which have greatly contributed to my academic journey.

Finally, my deepest gratitude also goes to all the people who have offered their help and support, whether from near or afar. I express my heartfelt thanks to everyone for your invaluable contributions to completing this dissertation.

Abstract

Connexins (Cx) are integral membrane proteins, they form gap junction channels (GJC) and hemichannels (HC) which are essential for brain functions. For a long time, astrocytes, which express Cx43, Cx26 and Cx30, have been known as a support to neuronal activity, but in the past twenty years the role of astrocytes in neurodegenerative diseases has gained recognition. During astrogliosis, the function of Cxs in astrocytes induces the opening of HCs, leading to neurotoxicity. Such pathological conditions can activate signalization pathways involving specific kinases, leading to the phosphorylation of Cxs therefore dysregulating GJC and HC activity.

The topology analysis allowed us to characterize the four transmembrane domains for Cx43, Cx26 and Cx30. Concerning the prediction of phosphorylation sites, our research confirmed that Cx43 phosphorylation sites cluster in its C-terminal (CT) end unlike Cx26 and Cx30. Our work revealed multiple phosphorylation sites for the first time. The most interesting ones could interfere with the regulating cytoplasmic loop (CL) and CT interaction which are S273, Y286 and T290 in the CT end for Cx43. S131 in the CL domain and S219, and S222 in the CT end for Cx26. T103 and S131 in the CL, and T227 in the CT end for Cx30. Finally, the comparative alignment of the three connexins uncovered features either shared between all three connexins or in pairs. Cx43, Cx26 and Cx30 shared S17 (S18 for Cx43) in the N-terminal (NT) and S85 (S86 for Cx43) in the second transmembrane domain. Sites shared between Cx26 and Cx30 are S5 in the NT which may influence the formation of the *NT plug*. S131 located in the CL neighbors the WW-motif which is responsible for heteromeric compatibility of connexons. S222 located in the CT end may be involved in the CL-CT interaction. These first-time predicted sites could have a role in dysregulating astrocytic GJC and HC, during neurodegenerative diseases.

Keywords: Gap junction, Cx43, Cx26, Cx30, Phosphorylation site, Prediction.

Résumé

Les connexines sont des protéines membranaires intégrales qui forment des jonctions communicantes et des hémicanaux essentiels aux fonctions cérébrales. Les astrocytes, qui expriment les Cx43, Cx26 et Cx30, sont connus depuis longtemps pour soutenir l'activité neuronale, mais au cours des vingt dernières années, le rôle des astrocytes dans les maladies neurodégénératives a été reconnu. Au cours de l'astrogliose, la fonction des connexines dans les astrocytes induit l'ouverture des hémicanaux, conduisant à une neurotoxicité. Ces conditions pathologiques peuvent activer des voies de signalisation impliquant des kinases spécifiques, conduisant à la phosphorylation des connexines et, par conséquent, à la régulation de l'activité des jonctions communicantes et des hémicanaux.

L'analyse topologique nous a permis de caractériser les quatre domaines transmembranaires pour la connexine 43, connexine 26 et connexine 30. Concernant la prédiction des sites de phosphorylation, notre recherche a confirmé que les sites de phosphorylation de la connexine 43 sont regroupés dans son extrémité C-terminale contrairement à la connexine 26 et la connexine 30. Notre travail a révélé pour la première fois des sites de phosphorylation dont certains pourraient interférer avec l'interaction entre la boucle cytoplasmique et l'extrémité C-terminale. Il s'agit de S273, Y286 et T290 dans l'extrémité C-terminale de la connexine 43. S131 dans la boucle cytoplasmique et S219, et S222 dans l'extrémité C-terminale pour la connexine 26, T103 et S131 dans la boucle cytoplasmique, et T227 dans l'extrémité C-terminale pour connexine 30. Enfin, l'alignement comparatif des trois connexines a mis en évidence des caractéristiques partagées entre les trois connexines ou par paires. Connexine 43, connexine 26 et connexine 30 partagent S17 (S18 pour Cx43) dans l'extrémité N-terminale et S85 (S86 pour connexine 43) dans le deuxième domaine transmembranaire. Les sites partagés entre connexine 26 et connexine 30 sont S5 dans l'extrémité N-terminale, ce qui peut influencer la formation du *NT plug*. S131, situé dans la boucle cytoplasmique, est voisin du motif WW responsable de la compatibilité hétéromérique des connexons. S222 situé à l'extrémité C-terminale peut être impliqué dans l'interaction boucle cytoplasmique-C-terminale. Ces sites prédits pour la première fois pourraient avoir un rôle dans le dérèglement des jonctions communicantes astrocytaires et des hémicanaux des maladies neurodégénératives.

Mots-clés : Jonction communicante, Cx43, Cx26, Cx30, Site de phosphorylation, Prédiction.

ملخص

الكونيكسيونات هي بروتينات غشائية، تشكل موصلات فجوية وقنوات نصفية، والتي تعتبر ضرورية لوظائف الدماغ. لوقت طويل، كان يُعرف أن الخلايا النجمية، التي تُعبّر عن كونكسين 43 وكونكسين 26 وكونكسين 30، انها تدعم النشاط العصبي. ولكن خلال العشرين عاماً الماضية، بدأ يُعترف بدور الخلايا النجمية في امراض التحلل العصبي. خلال عملية الدباق النجمي، يؤدي دور الكونيكسيونات في الخلايا النجمية إلى فتح القنوات النصفية، مما يؤدي إلى السمية العصبية. يمكن أن تُفعل هذه الظروف المرضية مسارات إشارات معينة تتضمن كينازات محددة، مما يؤدي إلى فسفرة الكونيكسيونات وبالتالي اختلال نشاط الموصلات فجوية والقنوات النصفية.

سمحت لنا تحليل الطوبولوجيا بتحديد أربع نطاقات عبر الغشاء لكل من كونكسين 43 وكونكسين 26 وكونكسين 30. فيما يتعلق بتنبؤ مواقع الفسفرة، أكدت أبحاثنا أن مواقع فسفرة كونكسين 43 تتجمع في نهاية الطرف الكربوكسيلي، على عكس كونكسين 26 وكونكسين 30. كشفت أبحاثنا عن مواقع فسفرة متعددة لأول مرة. من بين هذه المواقع الأكثر إثارة للاهتمام والتي يمكن أن تتداخل مع تفاعل الحلقة السيتوبلازمية والطرف الكربوكسيلي، والتي تشمل S273 و Y286 و T290 في الطرف الكربوكسيلي لـ Cx43. تشمل مواقع الفسفرة في مجال الحلقة السيتوبلازمية والطرف الكربوكسيلي لـ كونكسين 26 S131 و S219 و S222. أما بالنسبة لكونكسين 30، تشمل مواقع الفسفرة T103 و S131 في الحلقة السيتوبلازمية و T227 في الطرف الكربوكسيلي. أخيراً، كشفت مقارنة المحاذاة بين الكونيكسيونات الثلاثة عن ميزات إما مشتركة بين الكونيكسيونات الثلاثة أو بين زوجين منها. تشترك من كونكسين 43 وكونكسين 26 وكونكسين 30 في S17 (S18 لـ كونكسين 43) في النهاية الأمينية و S85 (S86 لـ كونكسين 43) في النطاق الغشائي الثاني. تشمل المواقع المشتركة بين كونكسين 26 وكونكسين 30 S5 في النهاية الأمينية، والتي قد تؤثر على تشكيل *NT plug*. S131 الموجود في الحلقة السيتوبلازمية يجاور *WW-motif*، المسؤول عن التوافق الهيتيروميري للكونيكسونات. يمكن أن يكون لـ S222 الموجود في الطرف الكربوكسيلي دور في تفاعل الحلقة السيتوبلازمية والطرف الكربوكسيلي. هذه المواقع المتنبأ لأول مرة قد تلعب دوراً في اختلال الموصلات فجوية والقنوات نصفية النجمية خلال امراض التحلل العصبي.

الكلمات المفتاحية: موصلات فجوية، كونكسين 43، كونكسين 26، وكونكسين 30، موقع الفسفرة، التنبؤ.

Table of Contents

Introduction	1
PartI Bibliographic Summary	4
ChapterI Connexins & Gap junctions	5
1) Connexins structure.....	6
2) Connexins form Gap Junctions	7
3) Gap junction function.....	10
4) Hemichannel and Gap Junction channels permeability	12
4.1 Regulation by Phosphorylation	12
4.2 Regulation by pH.....	14
4.3 Regulation by voltage.....	14
ChapterII Astrocytic Connexins.....	16
1) Astrocytes as Glial cells in the Central Nervous System.....	17
2) Astrocytic Connexins Expression and Function	18
3) Astrocytic Connexins and Neurodegenerative disease	18
3.1 Neurodegenerative diseases.....	18
3.2 Astrocytic Connexins in Neurodegenerative disease	19
PartII Experimental work and Results	21
ChapterIII Materials and methods	22
1) Topology prediction by ΔG predictor	23
2) Phosphorylation sites predictions by NetPhos	24
3) Protein alignment by Clustal Omega	26
4) Protein Visualisation by Protter	27
ChapterIV Results and Discussion	28

1) Topological analysis of Cx26, Cx30 and Cx43.....	29
2) Phosphorylation sites prediction of Cx43, Cx26 and Cx30	32
2.1 Connexin 43 phosphorylation prediction	33
2.2 Connexin 26 phosphorylation prediction	35
2.3 Connexin 30 phosphorylation prediction	36
3) Multisequence alignment of Cx43, Cx26 and Cx30	37
4) Domains and Predicted sites topology	39
4.1 Connexin 43 topology	39
4.2 Connexin 26 topology	40
4.3 Connexin 30 topology	41
Conclusion.....	45
References	48

Abbreviation List

cAMP:	Cyclic Adenosine-3',5'-Monophosphate
ATP:	Adenosine Triphosphate
Ca ²⁺ :	Calcium
CAM:	Cell Adhesion Molecules
Cdc2:	Cell Division Control 2
Cdk5:	Cyclin -Dependent Kinase 5
CKI:	Casein Kinase 1
CKII:	Casein Kinase 2
DNA-PK:	DNA-Dependent Protein Kinase
EGFR:	Epidermal growth factor receptor
GJC:	Gap junction channels
cGMP:	Cyclic Guanosine Monophosphate
GSK3:	Glycogen Synthase Kinase 3
HC:	Hemichannels
IP3:	Inositol Triphosphate
MAPK:	Mitogen-Activated Protein Kinase
PKA:	Protein Kinase A
PKB:	Protein Kinase B
PKC:	Protein Kinase C
PKG:	Protein Kinase G
RSK:	Ribosome S6 kinase

Table of Figures

Figure 1. 1: Connexin Topology in cell membrane.....	6
Figure 1. 2: Connexin units assemble into connexons and gap junction channels.....	9
Figure 1. 3: Gap junction channels and hemichannels in the cell membrane	10
Figure 1. 4: Cx26 permeability regulation through the formation of NT plug.....	15
Figure 2. 1: Glia-neuron interaction	17
Figure 2. 2: Schematic representation of Connexin expression in pathological conditions	20
Figure 3. 1: ΔG predictor user interface for “Full protein scan” mode.	24
Figure 3. 2: NetPhos 3.1 user interface	25
Figure 3. 3: Clustel Omega online server user interface.	26
Figure 3. 4: Jalview’s user interface.....	27
Figure 3. 5: Protter’s user interface.	27
Figure 4. 1: Hydropathy diagrams Provided by ΔG predictor for Cx43.	29
Figure 4. 2: Hydropathy diagrams Provided by ΔG predictor for Cx26.	30
Figure 4. 3: Hydropathy diagrams Provided by ΔG predictor for Cx30.	31
Figure 4. 4: Netphos 3.1 prediction results for Cx43	32
Figure 4. 5: Alignment of the three connexin isoforms.....	38
Figure 4. 6: Cx43 topology and phosphorylation sites visualization by Protter.....	40
Figure 4. 7: Cx26 topology and phosphorylation sites visualization by Protter.....	41
Figure 4. 8: Cx30 topology and phosphorylation sites visualization by Protter.....	42

List of Tables

Table 1. 1: Murine connexins	7
Table 1.2: Connexin phosphorylation effects on hemichannels permeability.....	13
Table 1.3: C43 Phosphorylation effect on Gap junction intercellular communication	14
Table 4. 1: Comparative table of the ΔG predictor results of the three connexins.....	31
Table 4. 2: Cx43 Predicted phosphorylation sites by NetPhos3.1.....	34
Table 4. 3: Cx26 Predicted phosphorylation sites by NetPhos3.1.....	35
Table 4. 4:Cx30 Predicted phosphorylation sites by NetPhos3.1	36

Introduction

Connexins are integral membrane proteins which have four-pass transmembrane domains and are named *tetraspans*. In the human genome they constitute a multigenic family of 21 isoforms. After synthesis connexins oligomerize into connexons, a protein complex of six connexin molecules, in the endoplasmic reticulum. Then they are translocated to the cell membrane, where they can either remain as "free" hemichannel anywhere on the plasma membrane or dock to another hemichannel to form a gap junction channel. These channels cluster together to form a junctional plaque (Willecke *et al.*, 2002)

Gap junction channels enable the passage of molecules such as ions, second messengers and metabolites of sizes around 1.8 kDa, between two adjacent cells. In the physiological state, channels constitute a critical component of cell-to-cell communication, enabling the coordination of electric and metabolic activities between cells (Wang *et al.*, 2004, Retamal *et al.*, 2015). Thus, gap junction channels maintain the liver's metabolic competence (Maes *et al.*, 2014), while in the heart these channels are crucial for facilitating the coordination and the synchronization of heartbeats (Sáez *et al.*, 2003).

Gap junction channels and hemichannels are essential for proper brain function as they allow electrical coupling of neurons as well as metabolic coupling of astrocytes and homeostasis. These glial cells provide trophic and metabolic support, regulate blood flow in response to neuronal activity, maintain extracellular homeostasis, and modulate synaptic activity. Recent studies suggest their involvement in complex brain functions like sleep, sensory processing and especially memory and cognitive functions (Koulakoff *et al.*, 2012).

In pathological states, the dysfunction of both gap junction channels and hemichannels is correlated with multiple diseases, like arrhythmias in the heart and neurodegenerative diseases in the central nervous system (Sáez *et al.*, 2003; Sanchez *et al.*, 2020). Historically, research into the pathogenesis of neurological disorders was focused on neurons and the role of astrocytes in these diseases was overlooked. In the last twenty years the role of astrocytes in the healthy and diseased brain has gained recognition (Huang *et al.*, 2021).

Alzheimer's disease is the leading cause of dementia among the elderly, while Parkinson's disease ranks as the second most common neurodegenerative disorder. Both conditions are marked by reactive astrogliosis, which involves morphological and functional changes in astrocytes (Stehberg *et al.*, 2012; Retamal *et al.*, 2014; Huang *et al.*, 2021).

During reactive astrogliosis, the expression and function of connexins in astrocytes change and induce the opening of hemichannels. These channels are thought to be responsible for the release of ions, metabolites and gliotransmitters (glutamate, ATP, etc) from astrocytes to insure brain functions and homeostasis (Orellana *et al.*, 2009). However, the excessive release of

glutamate is known to be neurotoxic, since it leads to the loss of synapses and to neuronal death (Huang *et al.*, 2021).

Studies on p38 α , a specific kinase from the MAPK family, have highlighted its role in response to various physiological and pathological conditions. In neurodegenerative diseases, p38 α is activated in response to environmental stresses including oxidative stress and inflammatory signals. This kinase phosphorylates several transcription factors as well as other kinases involved in particular signaling pathways. It has been proved that p38 α also phosphorylates structural proteins as tau protein leading to its hyperphosphorylation and to the formation of neurofibrillary tangles which are hallmarks of Alzheimer disease (Canovas and Nebreda, 2021). Since connexins are phosphoproteins, it may be possible that connexin phosphorylation status is also affected in response to oxidative stress via p38 α thereby disrupting gap junction and hemichannel activity, which draws our attention towards the importance of phosphorylation in astrocytic connexins (Pogoda *et al.*, 2016; Leithe *et al.*, 2018; Zhang *et al.*, 2023).

Our research aims to perform an *in silico* topology analysis using ΔG predictor (Hessa *et al.*, 2007) for three astrocytes connexins, Cx43, Cx26 and Cx30, then achieve a prediction of the post-translational modification, specifically the phosphorylation, of the three connexins using the *NetPhos 3.1* program (Hessa *et al.*, 2007). Finally, we conduct an alignment of the three proteins using *Clustal omega* (Madeira *et al.*, 2024) to detect common characteristic features among these three isoforms.

After a general introduction, highlighting the aims of our study, this manuscript consists of two parts:

The first part is a bibliographic summary consisting of two chapters:

- Chapter I presents general information on connexins, their structures, the formation of junctional channels and their regulation.
- Chapter II presents astrocytic connexins, their expression and function as well as their role in neurodegenerative diseases.

The second part is experimental and consists of two chapters:

- Chapter III explains the methods and tools used in this study
- Chapter IV presents the results obtained from the different methods applied during our work, their interpretation and a discussion.

Finally, this dissertation concludes with a general conclusion and perspectives.

Part I

Bibliographic Summary

Chapter I

Connexins & Gap junctions

1) Connexins structure

Connexins (Cxs) are membrane proteins which constitute a family of 21 isoforms encoded by the human genome. They are designated by Cx followed by their molecular weight in kDa ranging from 23 to 60 kDa. Thus, Cx43 the most expressed and studied one, possesses a molecular weight of 43 kDa (Beyer *et al.*, 1987). Connexins form gap junction channels, allowing paracrine signaling. As demonstrated by the study of Goodenough *et al.* (1996) using biochemical and sequence-specific antibody binding, Cx32, Cx26, and Cx43 share a common topology, as well as all the other connexins. These proteins have four hydrophobic helical transmembrane domains (TM1–4) which are connected through two extracellular loops (EL1 and EL2) and one cytoplasmic loop (CL). The N-terminal (NT) and C-terminal (CT) segments are also oriented to the cytosol (Goodenough *et al.*, 1996; Oviedo-Orta *et al.*, 2003; Retamal *et al.*, 2015; Kirichenko *et al.*, 2021) (**Figure 1.1**).

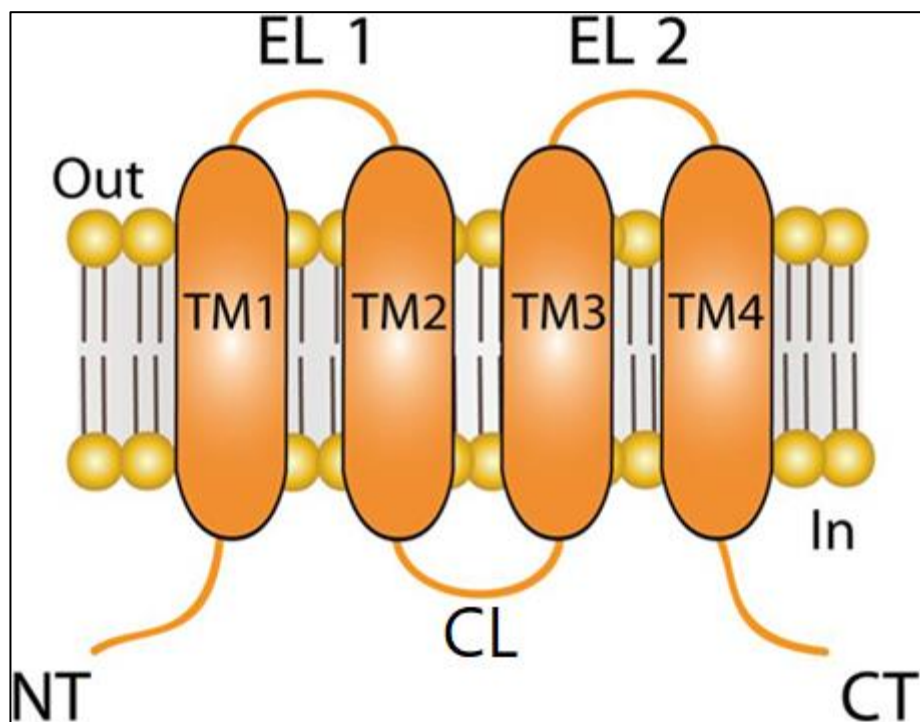


Figure 1. 1: Connexin Topology in cell membrane (Retamal *et al.*, 2015)

N-terminal (NT), C-terminal (CT), Cytoplasmic loop (CL), Extracellular loop (EL), Transmembrane domain (TM).

The length of cytoplasmic loops and C-terminal domains varies widely between connexin isoforms which are divided into five separate groups (alpha, beta, gamma, delta and epsilon) based on their structural homology (**Table1.1**).

Table 1. 1: Murine connexins (Adapted from Willecke et al., 2002)

Group	Connexins	Loop length (AA)	C-Terminal length (AA)
α	Cx37	55	105
	Cx40	55	135
	Cx43	44	155
	Cx46	50	190
	Cx50	50	210
β	Cx26	35	18
	Cx30	35	55
	Cx30.3	30	65
γ	Cx45	80	150
	Cx47	105	155
δ	Cx36	100	50
ϵ	Cx23	-	-

AA: Amino-acid

2) Connexins form Gap Junctions

Connexins oligomerize into hexameric structures (composed of six molecules) called *hemichannels* (HCs), also known as *connexons*. Each connexon is then delivered to the plasma membrane where it may dock to another connexon in the extracellular space to form a complete intercellular gap junction channel (GJC). Thus, connexins can form two types of channels, *single membrane channels* which remain as "free" HCs anywhere on the plasma membrane, and *two membrane-spanning channels* of neighboring cell membranes forming a continuous aqueous channel. The processes of oligomerization, transport and docking are crucial for the formation of gap junctions which is achieved by the clustering of intercellular channels into a junctional plaque with variable sizes that connects the cytoplasm of the two cells allowing

direct communication between adjacent cells (Goodenough *et al.*, 1996; Goodenough et Paul, 2009) (**Figure 1.2 A, B**) (Retamal *et al.*, 2015, Kirichenko *et al.*, 2021).

Most tissues express more than one connexin isoform. The oligomerization of six identical connexins forms a homomeric connexon, whereas if the connexins are different, the formed connexon is called heteromeric. The docking of two identical connexons creates a homotypic channel, but the docking of two different connexons creates a heterotypic channel (Figure 1.2 C) (Retamal *et al.*, 2015; Kirichenko *et al.*, 2021).

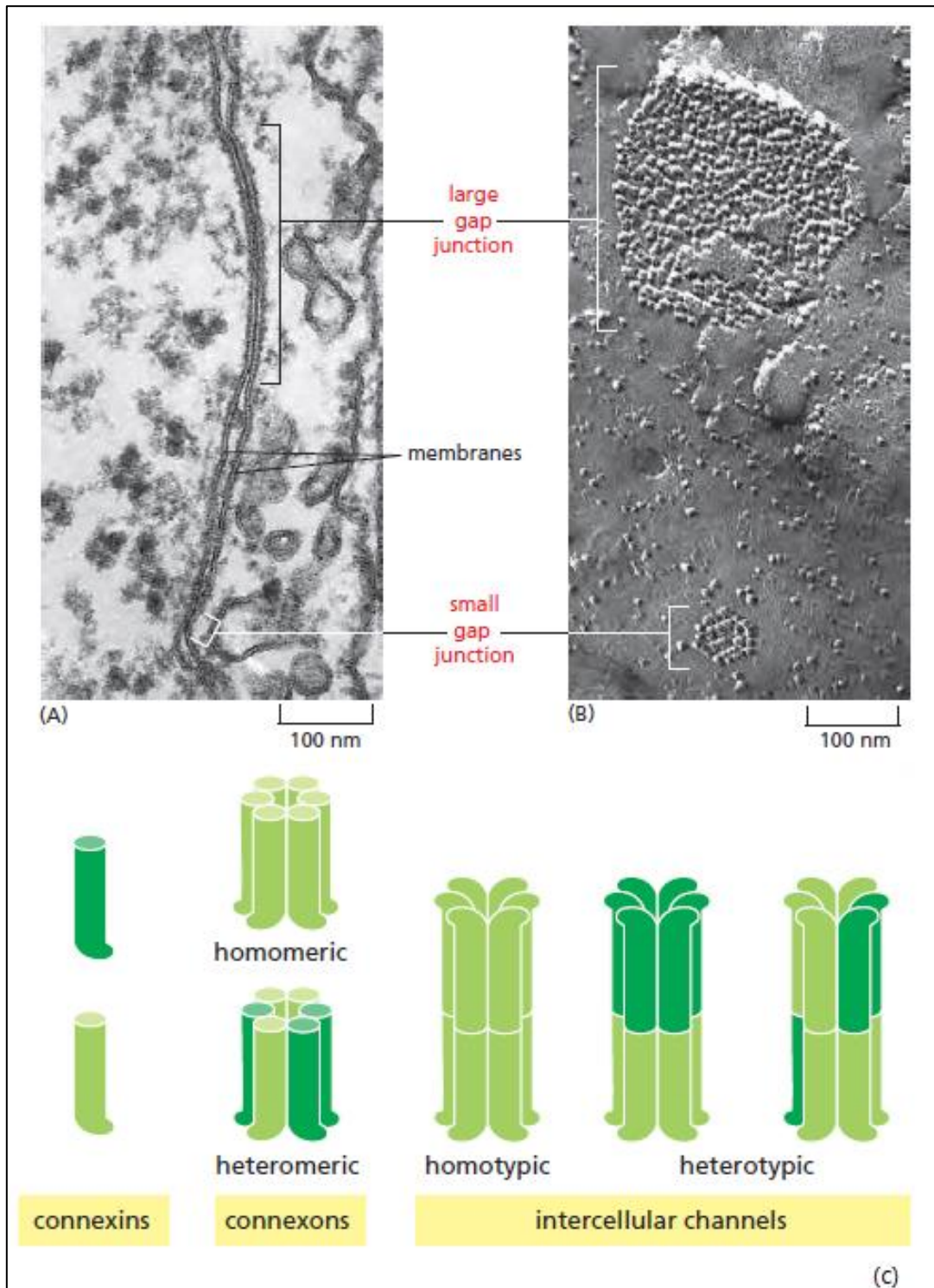


Figure 1.2: Connexin units assemble into connexons and gap junction channels

(A) Gap junction as seen in electron microscopy. (B) freeze-fracture electron micrographs of a large and a small gap junction plaque between fibroblasts. (C) The organization of connexins into connexons, and connexons into intercellular channels. The connexons can be homomeric or heteromeric, and the intercellular channels can be homotypic or heterotypic (Alberts *et al.*, 2015).

3) Gap junction function

Gap junction channels play crucial roles in intercellular signaling, as they allow the direct diffusion of small molecules with sizes around 1.8 kDa between adjacent cells. Conversely, HCs facilitate the release of some of these molecules into the extracellular space (**Figure 1.3**) (Orellana *et al.*, 2009; Pogoda *et al.*, 2016).

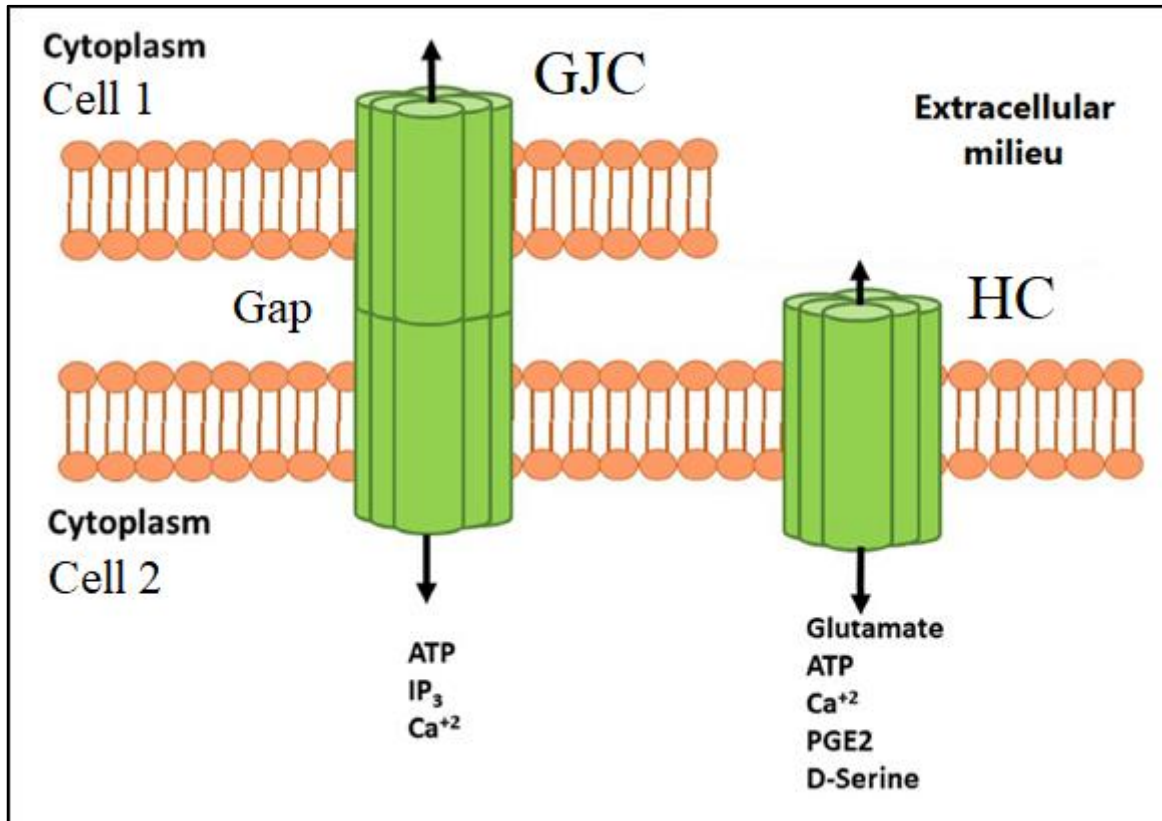


Figure 1. 3: Gap junction channels and hemichannels in the cell membrane

(Modified from Mayorquin *et al.*, 2018)

GJC: Gap junction channel; HC: Hemichannel; ATP: Adenosine triphosphate; IP₃: Inositol triphosphate; PGE₂: prostaglandin. Gap junction channels and hemichannels serve as channels for the transport of small molecules such as ions, second messengers, and metabolites between cells or between the cell and the extracellular milieu.

GJC are critical components of cell-to-cell communication, enabling the coordination of electric and metabolic activities between cells. The communication between these channels creates a pathway known as *gap junction intercellular communication* (GJIC), which facilitates passive diffusion of molecules between neighboring cells. The diffused molecules are second messengers like cyclic adenosine monophosphate (cAMP) and inositol triphosphate (IP₃), metabolites like adenosine 5'-triphosphate (ATP) and ions like calcium (Ca²⁺) (Wang *et al.*, 2004; Vinken *et al.*, 2011; Retamal *et al.*, 2015).

In the liver, most gap junctions are formed between hepatocytes, covering up to 3% of the hepatocellular membrane surface. Hepatocellular gap junctions are crucial for maintaining the liver's metabolic competence. Specifically, Cx32-based GJIC is essential for various liver-specific functions, including glycogenolysis, ensuring the distribution of metabolites and signaling molecules, thereby supporting metabolic functions and maintaining homeostasis (Maes *et al.*, 2014). In cardiac myocytes, gap junctions are located in specialized plasma membrane regions called *intercalated disks*, where the desmosome junctions which allow mechanical coupling between cells are also found. These GJC are crucial for allowing the intercellular passage of current-carrying ions, thereby facilitating the propagation of action potentials, thus ensuring the precise electric coordination of heartbeats (Sáez *et al.*, 2003).

Information HCs function is currently scarce, but some data suggest the implication of HCs in the release of signaling molecules (ATP, glutamate, prostaglandin) in certain cell types (Retamal *et al.*, 2015). Thus, astrocytes are implicated in the release of gliotransmitters (glutamate) which is critical for modulating neuronal activity and communication in the brain (Stehberg *et al.*, 2012). ATP released through HCs in myocytes signals adjacent cells by activating purinergic receptors, initiating the IP₃/IP₃ receptor pathway to propagate calcium signaling and coordinate cellular activities (Li *et al.*, 2012). Type II taste bud cells are involved in the perception of sweet, bitter, and umami tastes. The activation of these cells by tastant molecules leads to the release of ATP, which in turn activates neurons that convey the information to the brain (Kinnamon and Finger 2013; Retamal *et al.*, 2015).

Furthermore, the study of GJCs and HCs has significant implications for understanding and treating various diseases. Dysfunctional GJCs can lead to impaired electrical conduction in the heart, contributing to arrhythmias and other cardiac conditions. In the liver, disruptions in GJIC can affect metabolic processes and contribute to liver diseases. In Alzheimer's disease the activation of HCs in astrocytes surrounding amyloid plaques increases the release of ATP and glutamate, which can lead to neuronal calcium overload, synaptic depression, and ultimately neuronal damage (Sáez *et al.*, 2003; Maes *et al.*, 2014; Xing *et al.*, 2019; Sanchez *et al.*, 2020).

4) Hemichannels and Gap Junction channels permeability

The gating of gap junction channels and hemichannels is a complex process involving two states, *open* and *closed*. When the channel is open, it allows for the passive diffusion of molecules through its pore. Conversely, when the channel is closed, the pore is obstructed or occluded in some manner, preventing the passage of molecules, this also applies to HCs. This process is influenced by various stimuli, both internal and external, linked to physiological and pathological conditions and cell type. The stimuli include transmembrane potential difference (voltage), pH and calcium concentration (Peracchia, 2004).

The transmembrane potential difference regulation is complex since we may have two types of voltages, either the membrane voltage (V_m) or the junctional voltage (V_j). Cx voltage sensitivity is done through the presence of voltage-sensor amino acids affecting the conformation of these proteins. Therefore, this leads to the opening and closing of the channels (Bukauskas *et al.*, 2004; Oshima, 2014). Variations in pH induce conformational changes in connexins favoring the *Cytoplasmic Loop C-terminal Tail* (CL-CT) interaction, influencing channel gating (Leybaert *et al.*, 2017). Additionally, calcium ions act by binding to *calmodulin* (CaM), a calcium-binding protein, in a manner dependent on calcium concentration, i.e., higher calcium levels increase the affinity of calmodulin for connexins. CaM interaction with Cx influences their conformation and plays a critical role in modulating the gating of gap junction channels. Specifically, it regulates the transition between the channels' open and closed states, regulating GJIC (Peracchia, 2004).

Additionally, post-translational modifications like phosphorylation of connexins alter their charge, leading to conformational changes altering protein-protein interactions of connexins. This will modulate the junctional permeability which is crucial for cellular communication and consequently physiological processes (Pogoda *et al.*, 2016) due to mechanisms such as blockage by extracellular calcium and magnesium, negative membrane potential, and post-translational modifications of connexins. However, in pathological condition HCs can open under certain conditions such as lower pH, mechanical stimulation and also oxidative stress and inflammation, allowing communication between the intracellular and extracellular spaces (Xing *et al.*, 2019).

4.1 Regulation by Phosphorylation

Phosphorylation is the main post-translational modification that regulates many cellular mechanisms. It involves adding a phosphate group to serine (S), threonine (T), and tyrosine (Y) amino acid residues. This modification impacts the charge, hydrophily, and protein

structure, influencing the function of Cxs, and consequentially the junctional permeability. Connexins phosphorylation sites are located in the C-terminal tail for several isoforms (Aasen *et al.*, 2018; Leithe *et al.* 2018).

It has been demonstrated that the phosphorylation of Cx43, Cx35 (the fish ortholog of mammalian Cx36) and Cx36 in their C-terminal domain is correlated with the regulation of the permeability of the HCs they make (**Table 1.2**) (Pogoda *et al.*, 2016). However, Cx26 which possesses a short C-terminal domain, only 12 vs. 152 amino acids for Cx43, presents contradictory results regarding phosphorylation. Cx26 was initially described as a non-phosphoprotein (Traub *et al.*, 1989) but the work of Locke *et al.* (2009) revealed the presence of multiple phosphorylation sites within the C-terminal. Cx26 is also phosphorylated in its cytoplasmic loop (Pogoda *et al.*, 2016).

Table 1.2: Connexin phosphorylation effects on hemichannels permeability

(Adapted from Pogoda et al., 2016)

Kinases	Connexins	Phosphorylated residues	Effects on Hemichannels
PKA	Cx35/36	NA	reduced permeability
PKB	Cx43	Ser369, Ser373	increased permeability
	Cx26	NA	increased permeability
PKC	Cx43	Ser368	reduced permeability
MAPK	Cx43	serines 255, 262, 279, 282	reduced permeability

NA: Not applicable; Cx35/36: Cx35 is the fish ortholog of mammalian Cx36

Phosphorylation can also regulate channel properties by enabling the increase or decrease of gap junction intercellular communication. GJCs permeability regulation involves various kinases, serine/threonine kinases like protein kinase C (PKC), MAP kinase (MAPK), cAMP-dependent protein kinase A (PKA), and tyrosine kinases like Src (**Table 1.3**) (Pogoda *et al.*, 2016; Leithe *et al.*, 2018).

Table 1.3: Cx43 carboxy-terminal Phosphorylation effect on gap junction intercellular communication (Adapted from Pogoda *et al.*, 2016; Leithe *et al.*, 2018).

Kinases	Phosphorylated residues	Effects on GJIC
PKA	S364	increased
PKB	S369, S373	S373 phosphorylation increased GJIC
PKC	S368	decreased
MAPK	S255, S262, S279, S282	decreased
Src, Tyk2	Y247, Y265	reduced
CDK	S255, S262	?
CK1	S325, S328, S330	?
?	S296, S297, S306, S365, S372	?

4.2 Regulation by pH

The process involving pH is complex because it depends on the isoforms and the type of channel (HC, GJC), but in all cases, the molecular mechanism involved in channel closure implicates the CL-CT interaction. The analysis of Leybeart *et al.* (2017) shows that the permeability of GJC and HC formed from Cx43, Cx46 and Cx50 is affected with the CL-CT interaction. However, the best documented one is that of Cx43. Cx43's CL-CT interaction is facilitated under low pH conditions due to the increased α -helical order in a specific central region in the cytoplasmic loop named *L2 domain*. This region, which contains many positively charged amino acids, interacts with the sequence of nine amino acids at the C-terminal end, consequentially this interaction provokes channel obstruction (Leybeart *et al.*, 2017).

In contrast, Cx26 exhibits different behavior. At normal pH, CL-CT interactions occur, but upon acidification, protonated amino sulfonates like taurine interact with the CL and disrupt the CL-CT interaction, leading to the closure of both GJs and HCs (Locke *et al.*, 2011).

4.3 Regulation by voltage

The voltage sensitivity of channels formed by connexins is more complex than that of voltage-dependent channels (Na_v and K_v) that connect the intra- and extracellular environments; this is true for connexin HCs, where voltage sensitivity is membrane-bound (V_m). However, for GJCs, voltage sensitivity is termed junctional (V_j) because it connects the two cytosols of neighboring cells. The regulation of junctional permeability by voltage involves the N-terminal

domain and the interface between the first transmembrane segment and extracellular loop (TM1/EL1). The N-terminal domain, particularly the first 10 amino acids, plays a crucial role in connexin channel gating as it contains voltage-sensing amino acids. These studies suggest a conformational change in favor of the interaction between NT-TM1 and the closure of the channel in response to an electrical potential near the channel (Oshima, 2014; Bargiello *et al.*, 2017). Also, Oshima's 2014 work proposes a plug-gating model of Cx26 where the 3D structure was realized by Maeda *et al.* (2009), whereas the 6NT's of the connexon join together in a circular mean forming a hydrogen bonds network through D2 and T5, to make a funnel like plug constricting the pore to $\sim 14\text{\AA}$. Additionally the plug is stabilized via a hydrophobic interaction of W3 with M34 (**Figure 1.5**).

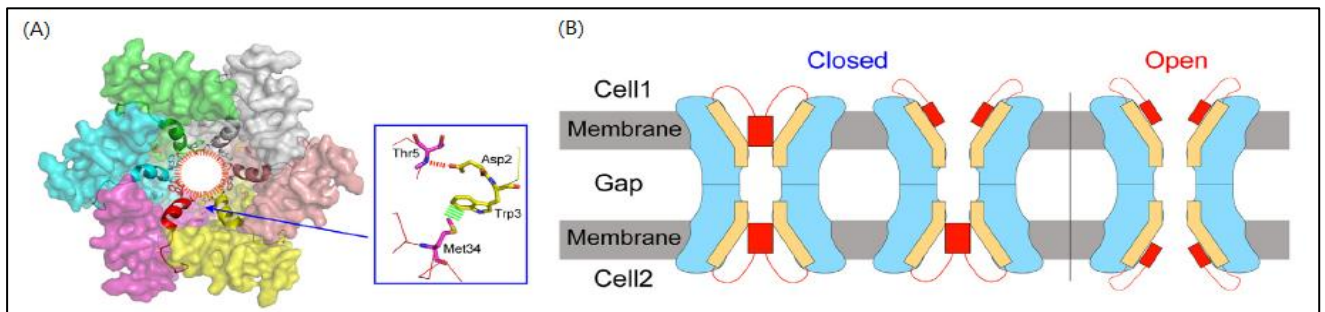


Figure 1.4: Cx26 permeability regulation through the formation of NT plug

(Oshima., 2014).

(A) Cx26 X-ray structure from the top demonstrating the NT plug formation by making a circular network of hydrogen bonds. (B) Hypothesized plug gating mechanism of gap junctions, each hemichannel (cyan) has its own plug formed by an assembly of N-terminals (red), allowing it to regulate its channel activity independently. The gap junction remains open only when the N-terminal in both hemichannels adopt an open conformation.

ChapterII

Astrocytic Connexins

1) Astrocytes as Glial cells in the Central Nervous System

In the central nervous system (CNS), neurons perform various functions such as receiving, integrating, processing, and propagating information. To accomplish these functions and survive, neurons require interaction with glial cells, which are astrocytes, oligodendrocytes and microglial cells. They provide essential support to neurons by offering trophic and metabolic assistance. They also contribute to the regulation of blood flow in response to neuronal activity, known as hyperemia, and maintain the homeostasis of the extracellular medium. Furthermore, astrocytes are involved in synaptic formation and activity. Recent studies suggest the involvement of these glial cells in complex brain functions such as sleep, sensory processing, memory and cognitive functions (**Figure 2.1**) (Allen and Barres 2009).

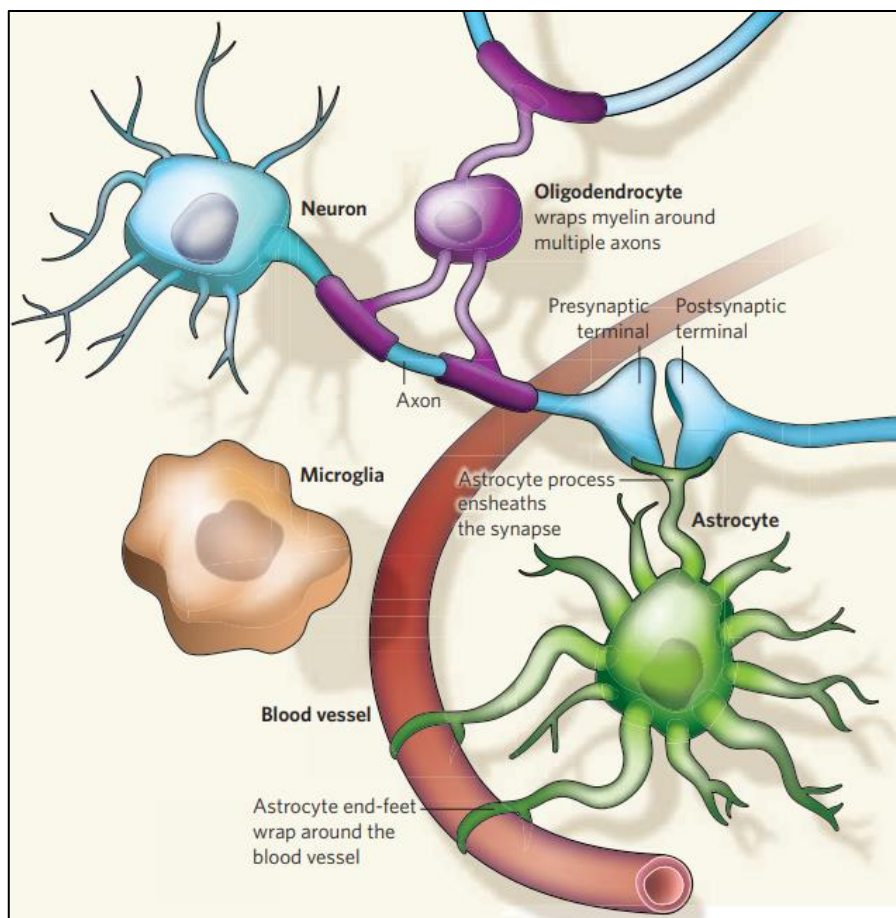


Figure 2.1: Glia-neuron interaction

(Allen and Barres, 2009)

2) Astrocytic Connexins Expression and Function

Astrocytes in the CNS are organized in tightly regulated plastic networks, primarily through Cxs which form either gap junctions creating a functional *syncytium* or hemichannels for paracrine signaling. This network plays a crucial role in maintaining CNS homeostasis and modulating neuronal activity. Metabolically, astrocytes in the brain and spinal cord are thought to contribute to extracellular K⁺ homeostasis, which is essential for proper neuronal function (Naggy *et al.*, 2000, Droguerre *et al.*, 2019, Xing *et al.*, 2019).

The expression of Cxs is detected in all cell types within the brain, with specific distribution and chronology. The molecular identity of Cxs varies among different glial cell types. Each cell type is characterized by a distinct set of Cx expressions, with more than one Cx often expressed within a defined cell type. Various Cxs have been detected through different experimental approaches, highlighting the complexity and specificity of Cx distribution in glial cells (Koulakoff *et al.*, 2012).

Astrocytes exhibit the highest level of Cx expression. The major astroglial connexins in adult astrocytes are predominantly Cx43 and Cx30 which are involved in the transport of glutamate glucose and lactic acid between astrocytes and neurons, facilitating local and distant communication. Additionally, Cx26 is also detectable in these cells (Koulakoff *et al.*, 2012, Xing *et al.*, 2019).

The expression of astrocytic connexins is tightly regulated and can vary depending on the developmental stage and physiological conditions. For instance, Cx43 is abundantly expressed in the astrocytes of the mature brain, while during brain development, the levels and distribution of Cx43 and Cx30 change. Also, in pathological states like in neurodegenerative diseases the levels and distribution of the astrocytic connexins fluctuate responding to various changes (Giaume *et al.*, 2010; Sanchez *et al.*, 2020).

3) Astrocytic Connexins and Neurodegenerative disease

3.1 Neurodegenerative diseases

Neurodegenerative diseases are a major threat to human health, especially for the geriatric population, as they involve the progressive loss of structure or function of neurons.

Alzheimer's disease (AD) is the most common neurodegenerative disorder, characterized by two hallmark features, the accumulation of extracellular amyloid plaques composed primarily of β -amyloid peptide (A β) and the accretion of intracellular neurofibrillary tangles composed of hyperphosphorylated species of microtubule-associated protein tau. Parkinson's disease (PD)

is the second most common neurodegenerative disorder, marked by the loss of dopaminergic neurons and the presence of Lewy bodies (LBs), which are intracytoplasmic neuronal inclusions of insoluble fibrillated aggregates that include α -synuclein (Erkkinen *et al.*, 2017; Sanchez *et al.*, 2020).

Historically, research into the pathogenesis of neurological disorders initially focused primarily on neurons, largely overlooking the role of astrocytes. Over the past twenty years, however, the importance of astrocytes in both healthy and diseased brains has gained significant recognition (Huang *et al.*, 2021).

3.2 Astrocytic Connexins in Neurodegenerative disease

During the pathogenesis of various neurodegenerative diseases, astrocytes undergo a process called reactive astrogliosis. This process is characterized by a morphological and functional remodeling of these cells. This remodeling is accompanied with changes in the expression and function of connexins, which are crucial for astrocyte communication and coordination with neurons (**Figure 2.2**).

In normal conditions, the permeability of Cx43 HC is low under resting conditions. However, in reactive astrocytes, this permeability is dysregulated due to pathological conditions such as ischemia, oxidative stress, inflammation, or increased free Ca^{2+} concentration. This dysregulation can lead to an imbalance in the transport of neurotransmitters and nutrients, contributing to neuronal dysfunction (Xing *et al.*, 2019; Huang *et al.*, 2021).

In Alzheimer's disease, increased opening of these channels might contribute to neuronal dysfunction. Studies have shown that cultured astrocytes treated with β -amyloid peptide result in the opening of astrocyte Cx43 hemichannels, leading to the release of ATP and glutamate and ultimately neuronal death (Orellana *et al.*, 2011). In Parkinson's disease mouse models, increased Cx43 expression and phosphorylation suggests that Cx43 may play a role in the pathogenesis of this neurodegenerative disease (Sanchez *et al.*, 2020).

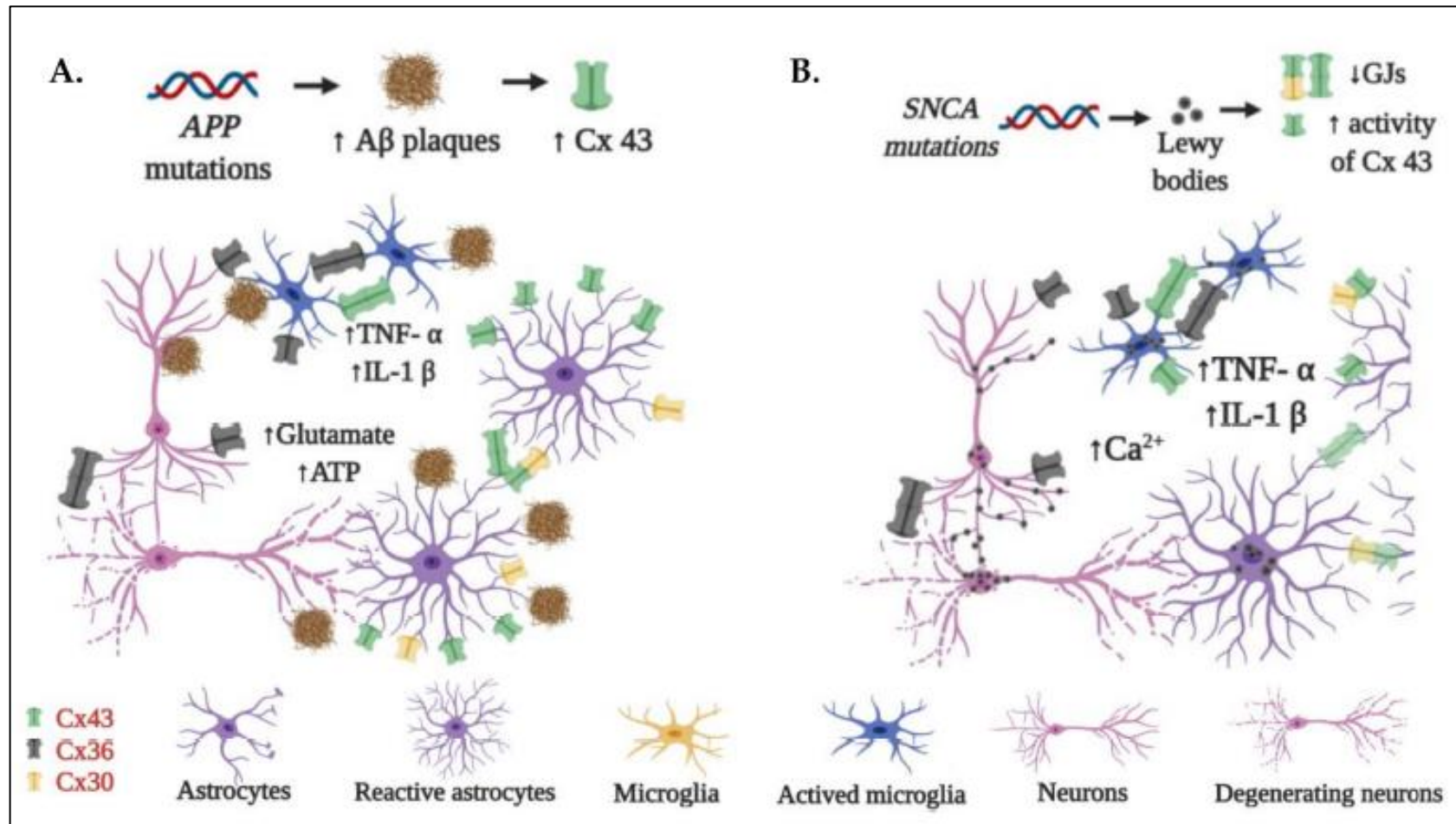


Figure 2.2: Schematic representation of Connexin expression in pathological conditions (Sanchez et al., 2020)

APP: Amyloid precursor protein; Aβ: β Amyloid; SNCA: α-synuclein; GJ: Gap junction; Cx: Connexin; TNF-α: Tumor necrosis factor; IL-1 β: Interleukin-1 beta.

(A) Connexin expression perturbation in Alzheimer's disease. Mutations in the APP gene lead to the accumulation of Aβ plaques, which are associated with increased levels of Cx43 and the chronic activation of Cx43 hemichannels which in turn leads to the excessive release of ATP and glutamate; (B) Connexin expression perturbation in Parkinson's disease. α-synuclein mutation leads to the aggregation of Lewy bodies lowering gap junction formation and increasing hemichannels activity.

PartII

Experimental work and

Results

Chapter III

Materials and methods

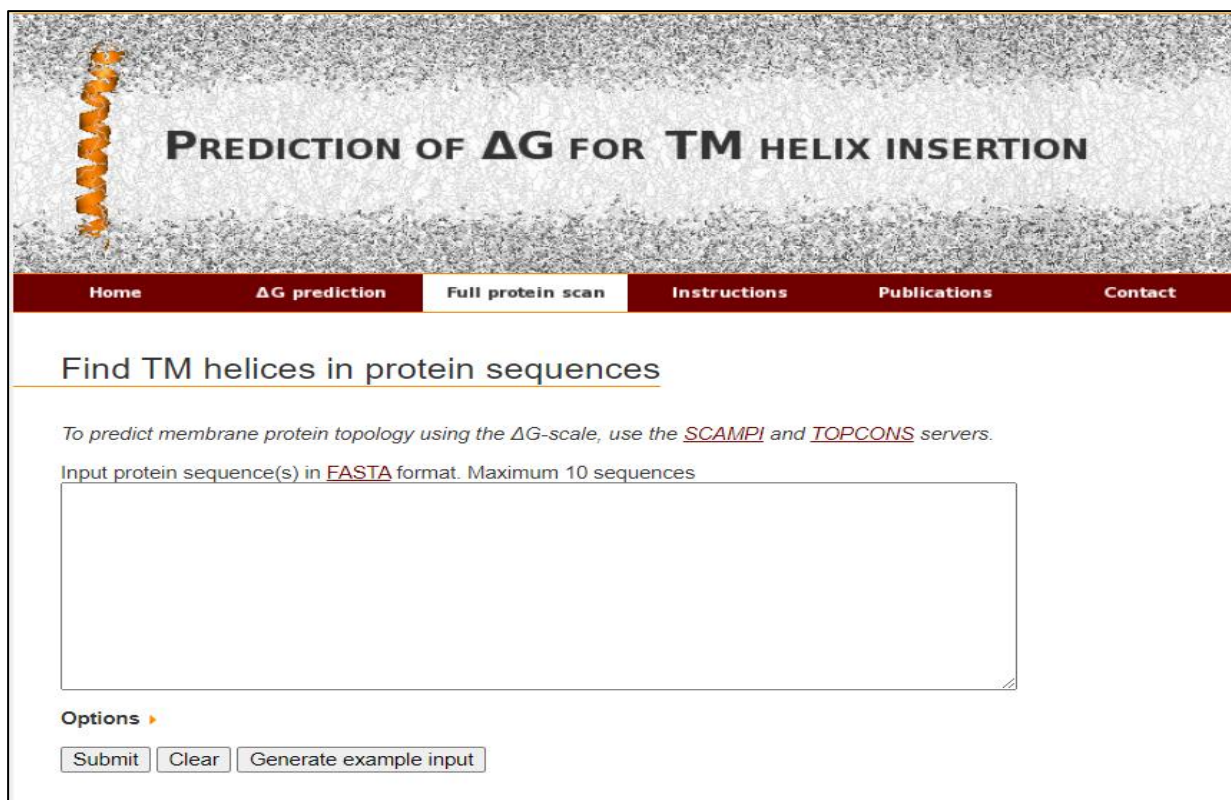
1) Topology prediction by ΔG predictor

We opted for *ΔG predictor server v1.0* for the topology prediction, because it offers a prediction based on the “biological scale” of Hessa *et al.* (2005), unlike most other topology programs which base their predictions on a purely “chemical scale” like the scale of Kyte and Doolittle (1982).

ΔG predictor is a prediction program that not only generates a two-dimensional graph, with ΔG_{app} values in the ordinate axis and position in sequence in the abscissa axis for different segment lengths, called a *hydrophobicity plot* according to the scale of Hessa *et al.* (2005) but also predicts a transmembrane segment in a protein sequence. Using the Sec61 translocon, these researchers quantitatively evaluated the insertion of segments into the endoplasmic reticulum membrane by studying the difference in apparent free energy (ΔG_{app}), where a negative value indicates that the sequence is recognized by the Sec61 translocon as a transmembrane sequence (transmembrane segment). The diagram plots these calculated ΔG_{app} values relative to the central position of the segment. Numerous overlaid graphs are generated by the server, scanning the sequence through a sliding window of varying lengths from 19 to 23 amino acids (Hessa *et al.*, 2007).

This program has two prediction modes, the first mode called “ ΔG prediction” used to identify potential transmembrane segments sequences, the second mode called “Full protein scan” which is used to predict the transmembrane segments found in a full protein sequence.

Since we used the program to predict the transmembrane domains of Cx26, Cx30 and Cx43, using their sequences in FASTA format obtained from Uniprot (www.uniprot.org), a protein sequence data bank, we used “Full protein scan” mode (<https://dgpred.cbr.su.se/index.php?p=fullscan>) (**Figure 3.1**).



The image shows a web interface for a protein prediction tool. At the top, there is a header with a textured background and a vertical orange helix icon on the left. The main title is "PREDICTION OF ΔG FOR TM HELIX INSERTION". Below the header is a navigation bar with six items: "Home", " ΔG prediction", "Full protein scan" (which is highlighted), "Instructions", "Publications", and "Contact". The main content area has a sub-header "Find TM helices in protein sequences". Below this, there is a paragraph of text: "To predict membrane protein topology using the ΔG -scale, use the [SCAMPI](#) and [TOPCONS](#) servers." followed by "Input protein sequence(s) in [FASTA](#) format. Maximum 10 sequences". There is a large empty text input box. Below the input box, there is an "Options" section with a dropdown arrow. At the bottom of the options section, there are three buttons: "Submit", "Clear", and "Generate example input".

Figure 3.1: ΔG predictor user interface for “Full protein scan” mode.

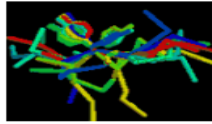
2) Phosphorylation sites predictions by NetPhos

In order to know potential phosphorylation sites of Cx26, Cx30 and Cx43, we used an online base server called *NetPhos 3.1* (<https://services.healthtech.dtu.dk/services/NetPhos-3.1/>) (Figure 3.2).

NetPhos - 3.1

Generic phosphorylation sites in eukaryotic proteins

The **NetPhos 3.1** server predicts serine, threonine or tyrosine phosphorylation sites in eukaryotic proteins using ensembles of neural networks. Both generic and kinase specific predictions are performed. The **generic** predictions are identical to the predictions performed by NetPhos 2.0. The **kinase specific** predictions are identical to the predictions by NetPhosK 1.0. Predictions are made for the following 17 kinases:



ATM, CKI, CKII, CaM-II, DNAPK, EGFR, GSK3, INSR, PKA, PKB, PKC, PKG, RSK, SRC, cdc2, cdk5 and p38MAPK.

Submission Instructions Output format PhosphoBase Downloads

Submission

Sequence submission: paste the sequence(s) and/or upload a local file

Paste a single sequence or several sequences in [FASTA](#) format into the field below:

Submit a file in [FASTA](#) format directly from your local disk:
 No file chosen

Residues to predict serine threonine tyrosine all three

For each residue display only the best prediction

Display only the scores higher than

Output format classical GFF

Generate graphics

Figure 3.2: NetPhos 3.1 user interface

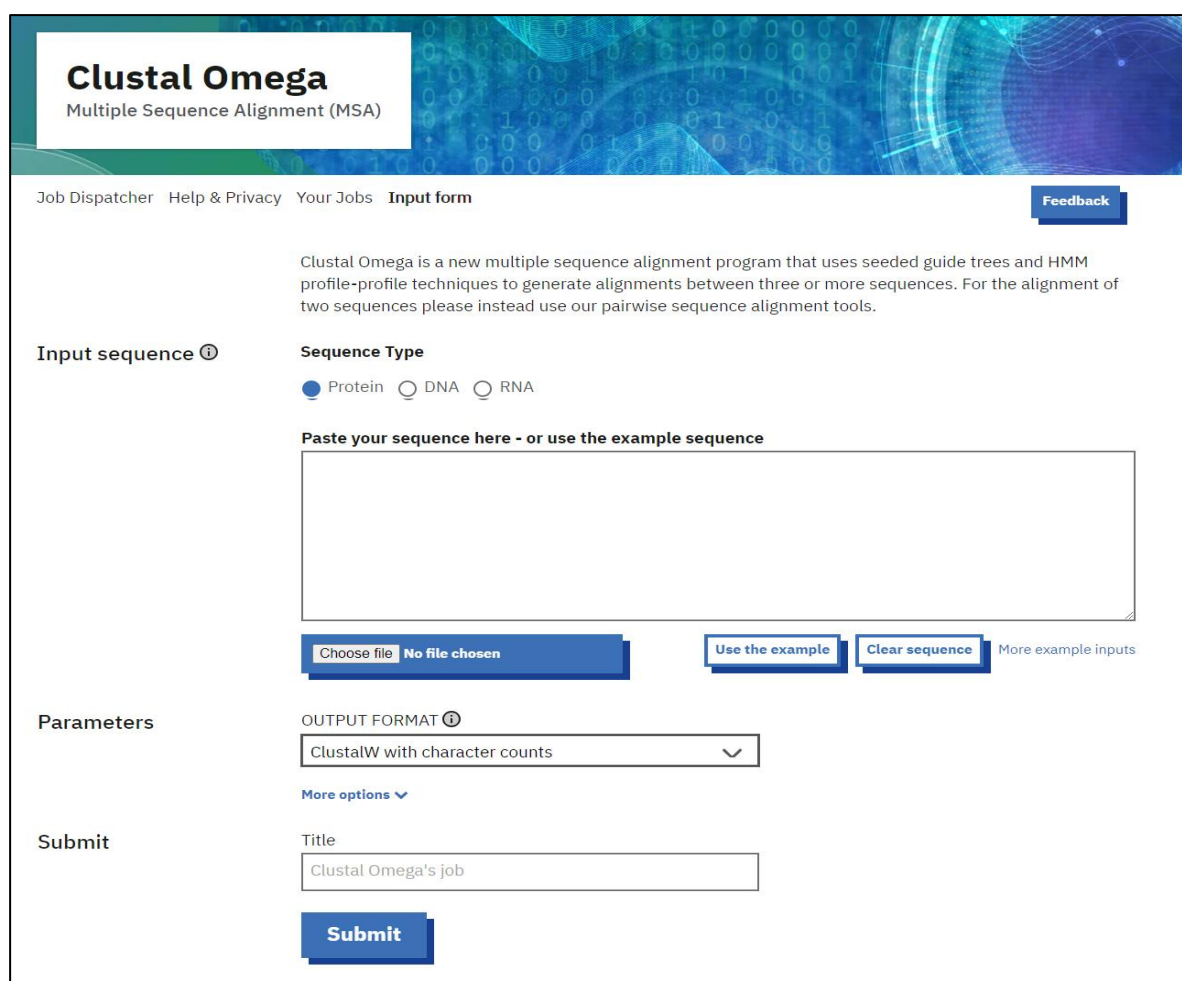
NetPhos 3.1, the most recent version of this program, benefits from an artificial neural network algorithm to predict phosphorylation sites of serine, threonine, or tyrosine. The web-based server can predict phosphorylation sites for a total of 17 kinases (ATM, CKI, CKII, CaM-II, DNAPK, EGFR, GSK3, INSR, PKA, PKB, PKC, PKG, RSK, SRC, cdc2, cdk5, and p38MAPK) (Blom *et al.*, 2004).

Although the interface allows customizing multiple settings, we only changed the “*Display only the scores higher than*” setting adjusting it to a “0.6” score. We then provided the FASTA sequence of each protein, obtained from UniProt, in different runs to get the prediction results.

3) Protein alignment by Clustal Omega

For the three proteins sequence alignment we used EMBL-EBI's Clustal Omega multiple sequence alignment online server (<https://www.ebi.ac.uk/jdispatcher/msa/clustalo>) (**Figure 2.4**) to identify regions of similarity that may indicate functional or structural relationships between the sequences.

Clustal Omega is a widely used multiple sequence alignment tool in bioinformatics. Although it is primarily designed for protein sequence alignment, Clustal Omega can also be used with nucleotide sequences (Madeira *et al.*, 2024).



The screenshot displays the Clustal Omega Multiple Sequence Alignment (MSA) web interface. At the top, the title 'Clustal Omega' is prominently displayed, followed by the subtitle 'Multiple Sequence Alignment (MSA)'. A navigation bar includes links for 'Job Dispatcher', 'Help & Privacy', 'Your Jobs', and 'Input form', along with a 'Feedback' button. A descriptive paragraph explains that Clustal Omega uses seeded guide trees and HMM profile-profile techniques for aligning three or more sequences, and suggests using pairwise tools for two sequences. The 'Input sequence' section features a 'Sequence Type' selector with radio buttons for 'Protein' (selected), 'DNA', and 'RNA'. Below this is a large text area for pasting sequences, accompanied by 'Choose file' (showing 'No file chosen'), 'Use the example', and 'Clear sequence' buttons, with a link to 'More example inputs'. The 'Parameters' section includes an 'OUTPUT FORMAT' dropdown menu set to 'ClustalW with character counts' and a 'More options' link. The 'Submit' section contains a 'Title' input field with the text 'Clustal Omega's job' and a 'Submit' button.

Figure 3.3: Clustal Omega online server user interface.

After providing the program with FASTA sequences of the three proteins Cx26, Cx30 and Cx43, the online server provides a result viewer, though for easier viewing and editing of the aligned sequences, we chose to view the results using *Jalview*, a free program which allows multiple sequence alignment editing, visualization and analysis (Waterhouse *et al.*, 2009) (**Figure 3.5**).



Figure 3.4: Jalview's user interface

4) Protein Visualization by Protter

Finally, we visually summarized our results using *Protter* (<http://wlab.ethz.ch/protter>) (Figure 3.6), an open-source tool designed for the visualization of proteoforms. Using Protter, we illustrated the different domains of our proteins and annotated the predicted phosphorylation sites, in order to communicate the essential aspects of our research (Omasits *et al.*, 2014).

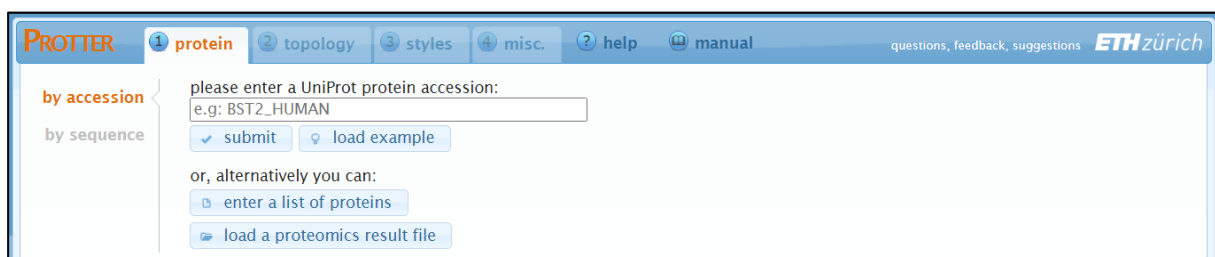


Figure 3.5: Protter's user interface.

ChapterIV

Results and Discussion

1) Topological analysis of Cx26, Cx30 and Cx43

In this study, we performed an analysis of the sequences Cx43 of α group and Cx26, Cx30 of β group which are usually expressed in astrocytes. The sequences provided from Uniprot data bank are used to characterize their transmembrane domains using the ΔG predictor program. The results are presented in the form of a diagram called a hydrophobicity plot. ΔG_{app} are values in the ordinate axis and position in sequence in the abscissa axis for different segment lengths. The hydrophobic regions of the hydrophathy profile present negative values of ΔG_{app} ; they correspond to the four helicoidal transmembrane domains TM1, TM2, TM3, and TM4 of these proteins. However, it should be noted that the N- and C-terminal and the cytoplasmic CL as well as the extracellular loops EL1 and EL2 segments are associated to positive values of ΔG_{app} . These results will allow us to predict the topology of the three connexins.

The analysis of the three diagrams provided by ΔG predictor shows the presence of four transmembrane domains. The predicted transmembrane segments TM1, TM2, TM3 and TM4 (**Figure 4.1A**) for Cx43 correspond to the sequences: $^{23}\text{K-V}^{41}$, $^{75}\text{V-A}^{94}$, $^{151}\text{L-I}^{172}$, $^{207}\text{T-F}^{229}$ respectively (**Figure 4.1B**).

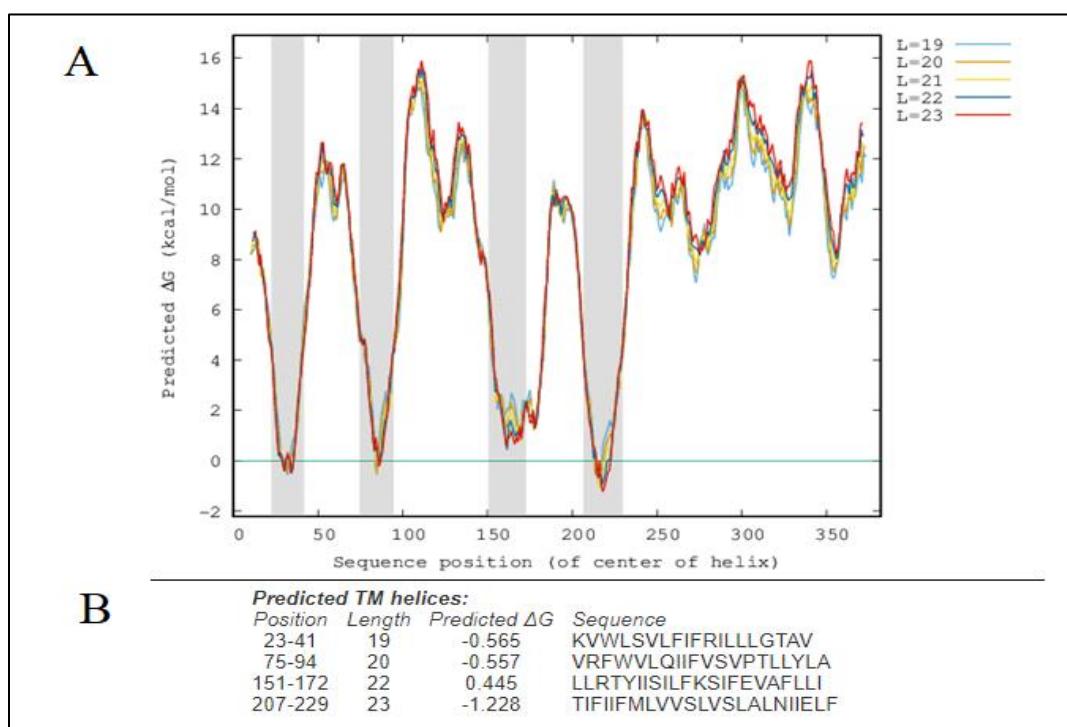


Figure 4.1: Hydrophathy diagrams provided by ΔG predictor for Cx43.

(A) The hydrophathy plot shows four major troughs highlighted with a gray strap signifying the four transmembrane domains; (B) Predicted transmembrane helices. The program provides for each transmembrane domain its position in the protein, the length of the predicted domain, its predicted ΔG and sequence

The predicted transmembrane segments TM1, TM2, TM3 and TM4 (**Figure 4.2A**) for Cx26 correspond to the sequences: $^{22}\text{K-W}^{44}$, $^{74}\text{I-M}^{93}$, $^{132}\text{L-F}^{154}$, $^{191}\text{F-L}^{213}$ respectively (**Figure 4.2B**).

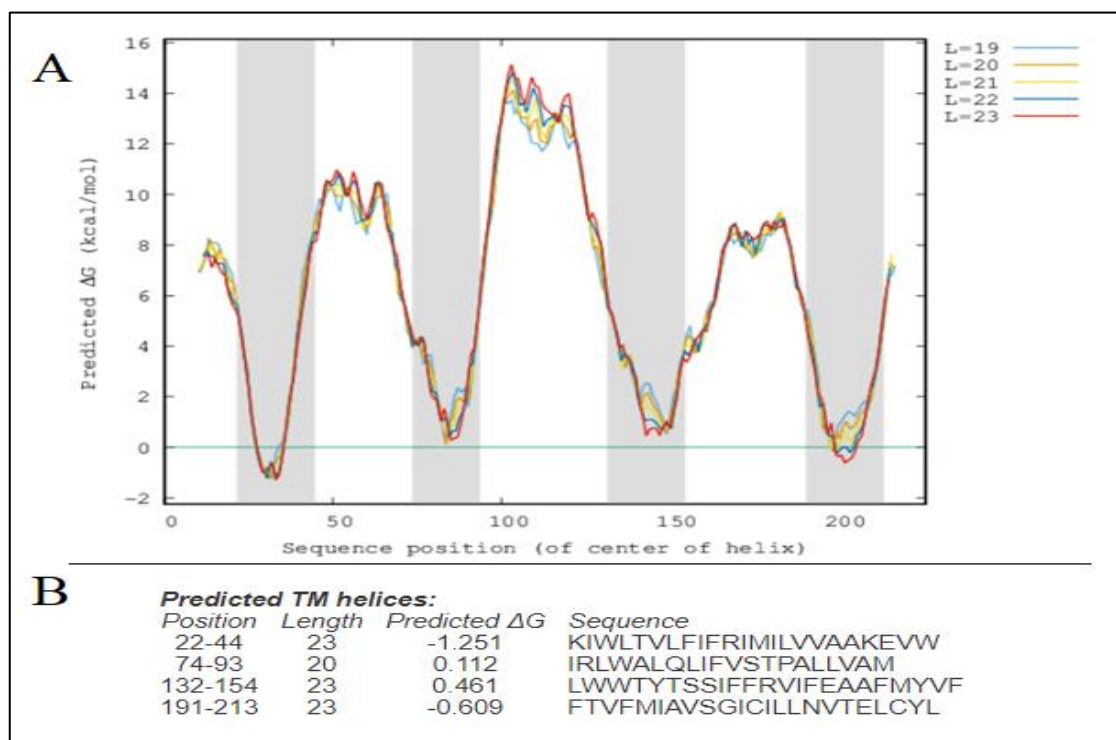


Figure 4.2: Hydropathy diagrams provided by ΔG predictor for Cx26.

(A) The hydropathy plot shows four major troughs highlighted with a gray strap signifying the four transmembrane domains; (B) Predicted transmembrane helices. The program provides for each transmembrane domain its position in the protein, the length of the predicted domain, its predicted ΔG and sequence

The predicted transmembrane segments TM1, TM2, TM3 and TM4 (**Figure 4.3A**) for Cx30 correspond to the sequences: $^{20}\text{I-A}^{40}$, $^{74}\text{I-M}^{93}$, $^{136}\text{Y-Y}^{158}$, $^{193}\text{I-L}^{215}$ respectively (**Figure 4.3B**).

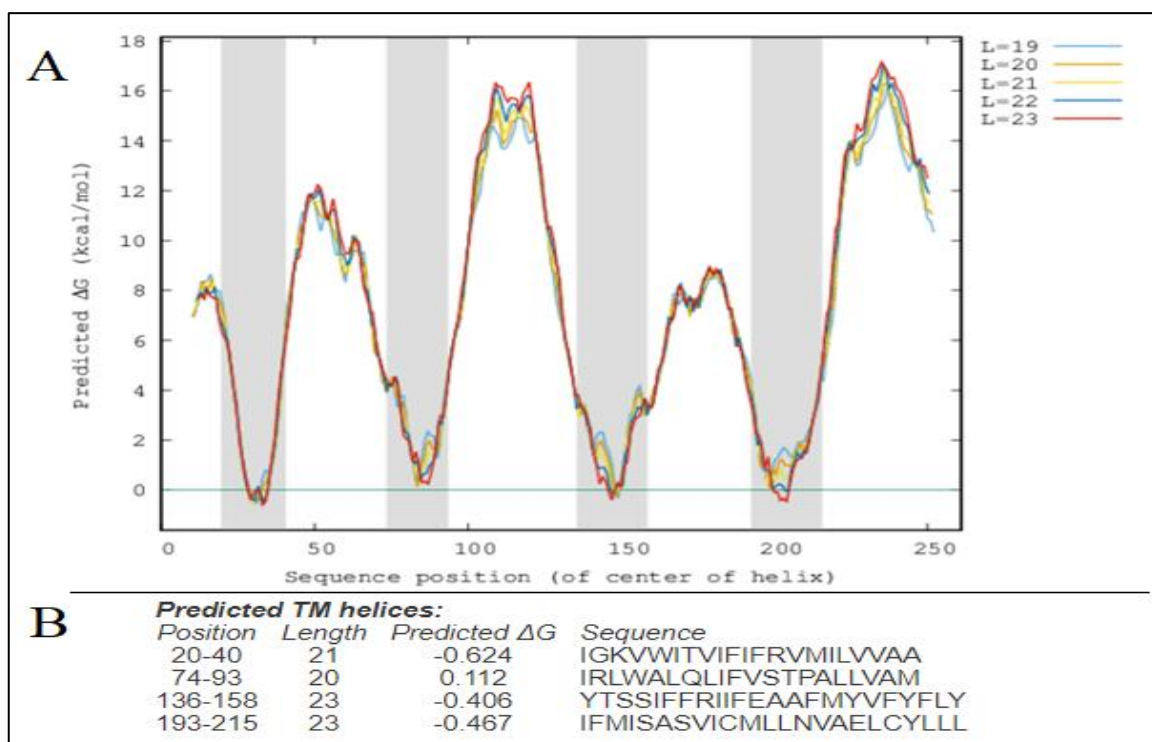


Figure 4.3: Hydropathy diagrams provided by ΔG predictor for Cx30.

(A) The hydropathy plot shows four major troughs highlighted with a gray strap signifying the four transmembrane domains; (B) Predicted transmembrane helices. The program provides for each transmembrane domain its position in the protein, the length of the predicted domain, its predicted ΔG and sequence

These results allowed us to characterize the different transmembrane domains for the three connexins Cx43, Cx26 and Cx30 which we compared below in **Table 4.1**.

Table 4. 1: Comparative table of the ΔG predictor results of the three connexins.

Group	Cx	NT	TM1	EL1	TM2	CL	TM3	EL2	TM4	CT
α	Cx43	1-22	23-41	42-74	75-94	95-150	151-172	173-206	207-229	230-382
β	Cx26	1-21	22-44	45-73	74-93	94-131	132-154	155-190	191-213	214-226
	Cx30	1-19	20-40	41-73	74-93	94-135	136-158	159-192	193-215	216-261

We split up the connexins into two groups, the first group α containing Cx43, and the second group β containing Cx26 and Cx30. It should be noted that the connexin protein family is divided into five groups which are α , β , γ , δ and ϵ where each Cx isoform is assigned a group

according to its protein length and its cytoplasmic loop length as well as its C-terminal length (Willecke *et al.*, 2002).

Evidently, we notice that Cx43 CL is about 55 amino acids long, and it is longer than the CL of both β group Cxs, Cx26 with 37 amino acids and Cx30 with 41 amino acids which only have an insignificant difference between them. That is also true for their C-terminals: we observe that Cx43 have a 152 amino acid C-terminal compared to the 45 amino acids long Cx30's C-terminal, and the shortest C-terminal of Cx26 with only 12 amino acids, which is consistent with the work of Willecke *et al.* (2002).

As for their N-terminals, extracellular loops and transmembrane domains, they practically have the same lengths with only very small differences no matter the group, α or β .

2) Phosphorylation sites prediction of Cx43, Cx26 and Cx30

In this work, we used another program, *NetPhos 3.1*, which allows for the prediction of potential phosphorylation sites based on the sequence for the three connexins Cx43, Cx26, and Cx30. The results of predicted phosphorylation sites are provided under the form of a sequence of nine amino acids centered around the phosphate acceptor site (P-4 S* P+4). Each result is associated with a probability score. The threshold value was set to 0.6 in our work with a few exceptions.

Netphos 3.1 results are presented in a table, where Uniprot identifier is used to name each connexin, for example “p17302_CXA1_HUMAN” is the identifier for Cx43. For each amino acid residue (x) of the sequence, Netphos provides its position indicated with #, the type of phosphorylated amino acid with T/S/Y. The sequence containing the predicted site is also given as well as possible kinases which may be responsible for this phosphorylation. The program only approves predictions with scores higher than 0.5, labeling them with “YES”, otherwise it labels them with “.” (Figure 4.4).

```

>sp_P17302_CXA1_HUMAN 382 amino acids
#
# netphos-3.1b prediction results
#
# Sequence          # x  Context    Score  Kinase  Answer
# -----
# sp_P17302_CXA1_HUMAN  18 S  VQAYSTAGG  0.663  unsp   YES
#
# sp_P17302_CXA1_HUMAN  86 S  IIFVSVPTL  0.693  PKA    YES
#
# sp_P17302_CXA1_HUMAN 180 S  IYGFSLSAV  0.603  PKA    YES
#
# sp_P17302_CXA1_HUMAN 186 T  SAVYTCKRD  0.867  PKC    YES
#
# sp_P17302_CXA1_HUMAN 186 T  SAVYTCKRD  0.796  unsp   YES

```

Figure 4.4: Netphos 3.1 prediction results for Cx43

The prediction results are given in **Table 4.2** for Cx43, in **Table 4.3** for Cx26 and in **Table 4.4** for Cx30.

2.1 Connexin 43 phosphorylation prediction

Netphos 3.1 predicted 24 phosphorylation sites for Cx43 with scores ranging from 0.6 to 0.9 (**Table 4.2**). Cx43 is known to be a phosphoprotein with at least 18 confirmed phosphorylation sites in the C-terminal region (Leithe *et al.*, 2018). Netphos 3.1 predicted 15 sites (marked with “+”) of which the majority have high scores of 0.8 or higher, are highlighted in red, and are experimentally confirmed to be phosphorylated with several kinases. These sites are Y247 and Y265 (Src); S364 (PKA); S369 and S373 (PKB); S368 (PKC); S255, S262, S279 and S282 (MAPK); S255 and S262 (CDK) and S325, S328 and S330 (CKI). For most of these predictions Netphos 3.1 did not successfully predict the correct kinase, otherwise it suggests another kinase. The kinase was predicted correctly only for S368 with PKC. However, the three experimentally confirmed sites S297, S328, and S330 were not predicted (**Table 1.3**) (Leith *et al.*, 2018).

It is interesting to note that our work predicted phosphorylation sites of the three connexins for the first time. These sites are S18 at the N-terminal domain, S86 in the second transmembrane domain (TM2) and two sites, S180 and T186 in the second extracellular loop (EL2), and five sites S244, S273, Y286, T290, and S344 in addition to three sites, and in the C-terminal domain.

The higher probability predictions matching with the experimentally determined results reaffirm the reliability of the program, which makes the experimentally unidentified sites an interesting target for testing.

Table 4.2: Cx43 Predicted phosphorylation sites by NetPhos3.1

	Site	Kinase	Sequence	Score	Experimentally confirmed
NT	S18	unsp	VQAYS*TAGG	0.663	-
TM2	S86	PKA	IIFVS*VPTL	0.693	-
EL2	S180	PKA	IYGFS*LSAV	0.603	-
	T186	PKC	SAVYT*CKRD	0.867	-
CT	S244	unsp	VKGRS*DPYH	0.833	-
	Y247	unsp	KSDPY*HATS	0.819	+ / Src; Tyk2.
	S255	unsp	SGALS*PAKD	0.989	+ / MAPK; CDK1.
	S262	PKC	KDCGS*QKYA	0.838	+ / MAPK; CDK1.
	Y265	unsp	GSQKY*AYFN	0.620	+ / Src; Tyk2.
	S273	unsp	NGCSS*PTAP	0.849	-
	S279	unsp	TAPLS*PMSP	0.978	+ / MAPK
	S282	unsp	LSPMS*PPGY	0.975	+ / MAPK
	Y286	unsp	SPPGY*KLVT	0.919	-
	T290	PKC	YKLV*GDRN	0.732	-
	S296	unsp	DRNNS*SCRN	0.983	+
	S306	unsp	NKQAS*EQNW	0.610	+
	S325	PKC	GQAGS*TISN	0.871	+ / CK1
	S344	unsp	DNQNS*KKLA	0.788	-
	S364	PKC	DQRPS*SRAS	0.824	+ / PKA
	S365	unsp	QRPSS*RASS	0.995	+
	S368	PKC	SSRAS*SRAS	0.862	+ / PKC
	S369	unsp	SRASS*RASS	0.995	+ / PKB
	S372	PKC	SSRAS*SRPR	0.887	+
	S373	unsp	SRASS*RPRP	0.997	+

Unsp: Unspecified; The phosphorylation sites are shown in red with an asterisk; Scores higher than 0.8 are shown in red. Experimentally confirmed sites and their kinases were obtained from Axelsen *et al* (2013), Pogoda *et al* (2016), Leithe *et al* (2018) and Zhang *et al* (2023).

2.2 Connexin 26 phosphorylation prediction

Our prediction using NetPhos3.1 presents 10 phosphorylation sites for Cx26 (**Table 4.3**). Unlike Cx43 which is hyperphosphorylated, Cx26 was identified as non-phosphoprotein (Traub *et al.*, 1989), until it was proven otherwise by the work of Locke *et al.* (2009) which showed five potential phosphorylation sites for Cx26. Three of these sites has been predicted by NetPhos 3.1 (marked by “+”) which are the sites T5 in the N-terminal domain with a score lower than 0.6, but we have kept in the results because it presents a potential phosphorylation site proposed by Locke *et al.* (2009). The two other sites are T123 in the cytoplasmic loop domain and T186 in the second extracellular loop which are predicted with high scores that are superior to 0.9. The remaining two, which has been described in the work of Locke *et al.* (2009), T8 and S183, were not predicted by our work.

Our results also predicted sites for the first time which are S17 in the N-terminal region, T26 in the first transmembrane domain, S85 in the second transmembrane domain, T123 in the cytoplasmic loop region, S162 in the second extracellular loop region, S222 and S219 in the C-terminal region.

Table 4.3: Cx26 Predicted phosphorylation sites by NetPhos3.1

	Site	Kinase	Sequence	Score	Potential phosphorylation sites
NT	T5	DNAPK	MDWGT*LQTI	0.548	+
	S17	unsp	VNKHS*TSIG	0.854	-
TM1	T26	PKC	KIWLTVLFI	0.640	-
TM2	S85	PKA	LIFVSTPAL	0.648	-
CL	T123	unsp	EEIKT*QKVR	0.923	+
	S131	PKA	RIEGSLWWT	0.682	-
EL2	S162	unsp	YDGFS*MQRL	0.750	-
	T186	unsp	VSRPT*EKTV	0.924	+
CT	S219	PKC	IRYCS*GKSK	0.910	-
	S222	unsp	CSGKS*KKPV	0.789	-

Unsp: Unspecified; The phosphorylation site is shown in red with an asterisk; Scores higher than 0.8 are shown in red. Potential phosphorylation sites were obtained from Locke *et al.* (2009).

2.3 Connexin 30 phosphorylation prediction

For Cx30, Netphos 3.1 has predicted 13 phosphorylation sites with scores ranging from 0.6 to 0.9 (**Table 4.4**). The work of Alstrøm *et al.* (2015) highlighted the PKC phosphorylation of seven sites in *xenopus laevis* Cx30, five of them were consistent with our prediction (marked by “+”). The predicted sites are T5, T8, T102, S222 and S239. The two other S225 and S258 were not, because they correspond to the Cx30 sequence of *xenopus laevis* and they are not conserved in the human Cx30, where they are substituted alanine (A255) and glutamine (Q258).

For Cx30, Netphos 3.1 has also predicted the first time the sites S17 and T18 in the N-terminal domain, S85 in the second transmembrane domain, T103 and S131 in the cytoplasmic loop domain, T186 in second extracellular domain, S199 in the fourth transmembrane domain and T227 in the C-terminal domain.

Table 4.4: Cx30 Predicted phosphorylation sites by NetPhos3.1

	Site	Kinase	Sequence	Score	Experimentally confirmed
NT	T5	CKI	MDWG T *LHTF	0.515	+ / PKC
	T8	PKC	GTLH T *FIGG	0.575	+ / PKC
	S17	unsp	VNKH S *TSIG	0.854	-
	T18	PKC	NKH S *SIGK	0.616	-
TM2	S85	PKA	LIFV S *TPAL	0.648	-
CL	T102	PKC	YRHET T *TRKF	0.835	+ / PKC
	T103	unsp	RHET T *RKFR	0.807	-
	S131	PKA	RIEG S *LWWT	0.706	-
EL2	T186	unsp	ISRPT T *EKTV	0.926	-
TM4	S199	PKC	MISAS S *VICM	0.622	-
CT	S222	PKC	CFRR S *KRAQ	0.874	+ / PKC
	T227	PKC	KRAQT T *QKNH	0.874	-
	S239	PKA	ALKE S *KQNE	0.676	+ / PKC

Unsp: Unspecified; The phosphorylation site is shown in red with an asterisk; Scores higher than 0.8 are shown in red. Experimentally confirmed phosphorylation sites and their kinase PKC were obtained from Alstrøm *et al* (2015).

3) Multisequence alignment of Cx43, Cx26 and Cx30

The analysis of the alignment provided by Clustal Omega viewed in Jalview shows that the three connexins, one from α group Cx43 and the two β group Cx26 and Cx30, share seven common phosphorylation sites (**Figure 4.5**). Two instances where all of them share the same predicted phosphorylation sites, S17 (S18 for Cx43) in their N-Terminal domains and S85 (S86 for Cx43) in each of their TM2 domains. Four instances where the two isoforms Cx26 and Cx30 share common predicted sites, T5 S131, T186 and S222. And strangely Cx26 of group β shares a common predicted phosphorylation site with only Cx43 of group α at S162 (S180 for Cx43).

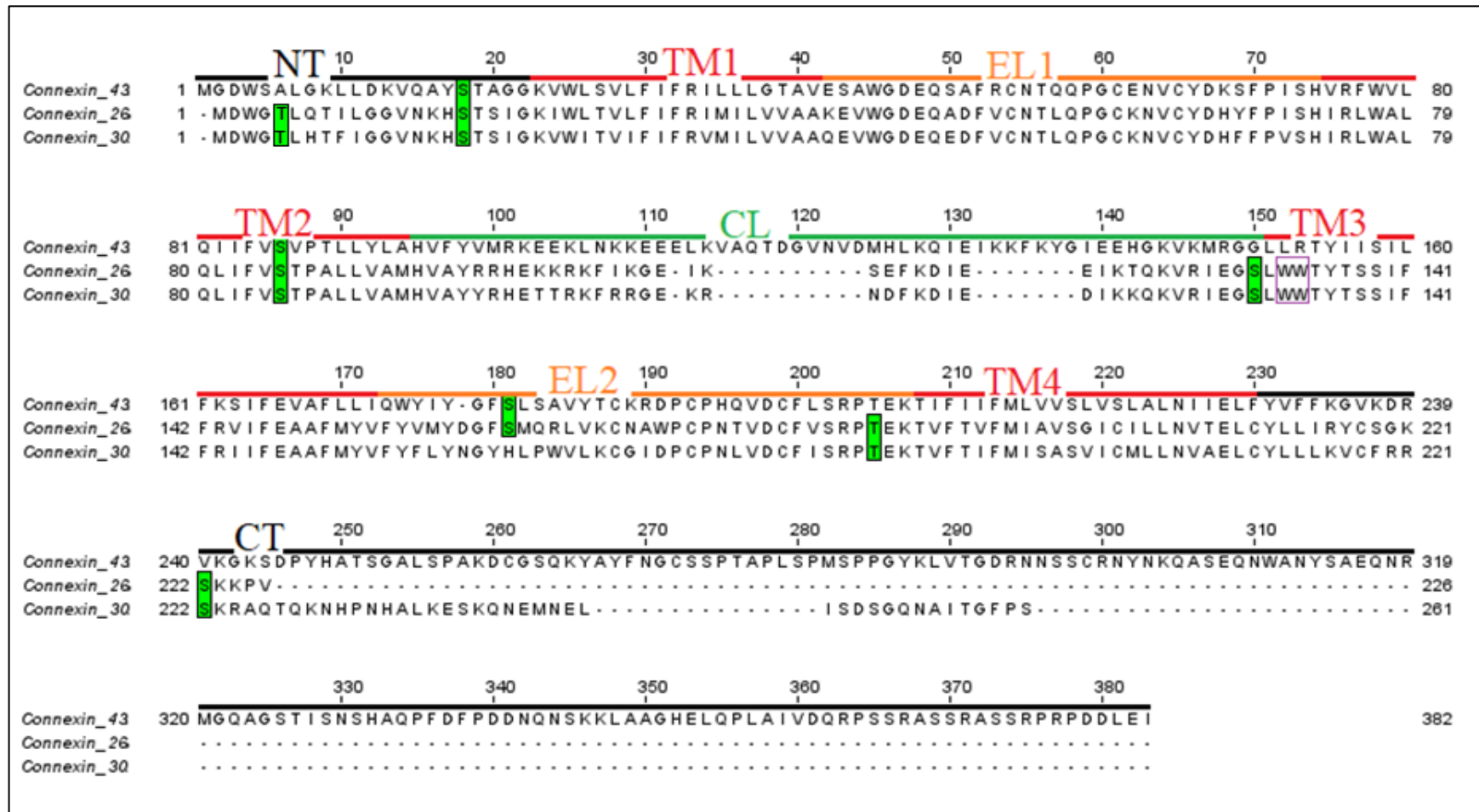


Figure 4.5: Alignment of the three connexin isoforms

The different domains, NT: N-terminal; TM: transmembrane; EL: Extracellular loop; CL: Cytosolic loop; CT: C-Terminal, indicated above in the MSA correspond to the results of the ΔG predictor for Cx43. Common predicted phosphorylation sites are highlighted in green and the WW-motif is in a purple border.

4) Membrane topology of connexins and predicted phosphorylation sites

Using the Protter program, we mapped the topology of Cx43, Cx26 and Cx30 based on results we got from ΔG Predictor. This allowed us to illustrate the predicted transmembrane domains. The predicted phosphorylation sites are provided by NetPhos 3.1. The topology analysis of Cx43, Cx26 and Cx30 reaffirms the typical connexin structure, featuring four transmembrane domains, cytosol-exposed N- and C-terminal domains, a cytoplasmic loop connecting TM2 and TM3, and two extracellular loops EL1 connecting TM1 and TM2, and EL2 connecting TM3 and TM4.

4.1 Connexin 43 topology

Protter presents the topology of Cx43 in the cell membrane, with the usual connexin structure. This connexin seems to have a large C-terminus domain, and even extracellular loops.

Unlike the experimentally confirmed predicted sites (shown in green) which are focalized in the C-terminal domain, the first-time predicted sites (shown in blue) are found all over the protein domains. These newly found sites are S18 in the N-terminal region and S86 in the second transmembrane domain, which Cx43 shares with Cx26 and Cx30 as predicted phosphorylation sites (represented by a diamond shape). Also, S180 in the second extracellular loop shared as a predicted phosphorylation site with Cx26 (represented by a square shape). Additionally, T186 in the second extracellular loop and S273, Y283, T290 and S344 in C-terminal region were uniquely predicted for Cx43 (**Figure 4.6**).

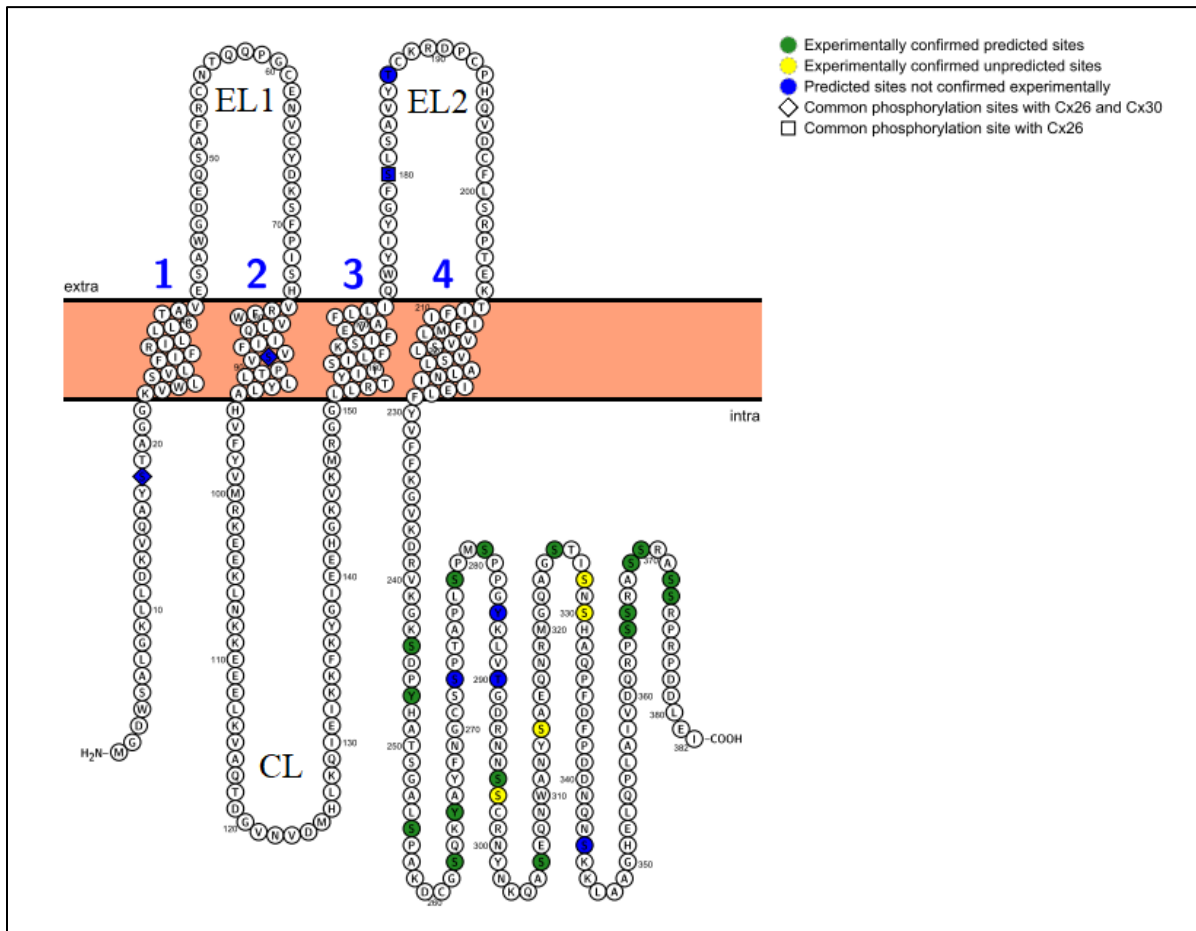


Figure 4.6: Cx43 topology and phosphorylation sites visualization by Protter.

4.2 Connexin 26 topology

Protter shows that Cx26 presents a particular topology characterizing its small C-terminal region (12 amino acids) which is even smaller than its N-terminal region (21 amino acids). Also, its second extracellular loop (35 amino acids) is bigger than its first extracellular loop (28 amino acids).

Netphos 3.1 has predicted sites in Cx26 in different regions of the protein, experimentally proposed and predicted sites (shown in green), and first-time predicted sites (shown in blue). These predicted sites are either shared with Cx43 and Cx30 (represented with a diamond shape) these are S17 in the N-terminal region and S85 in the second extracellular domain, or a shared site with only Cx43 (represented by a square shape and written in red) which is S162, or shared sites with only Cx30 which are T5 in the amino-terminal domain, S131 in the cytoplasmic loop, S162 in the second extra cellular loop and S222 in the C-terminal domain (**Figure 4.7**).

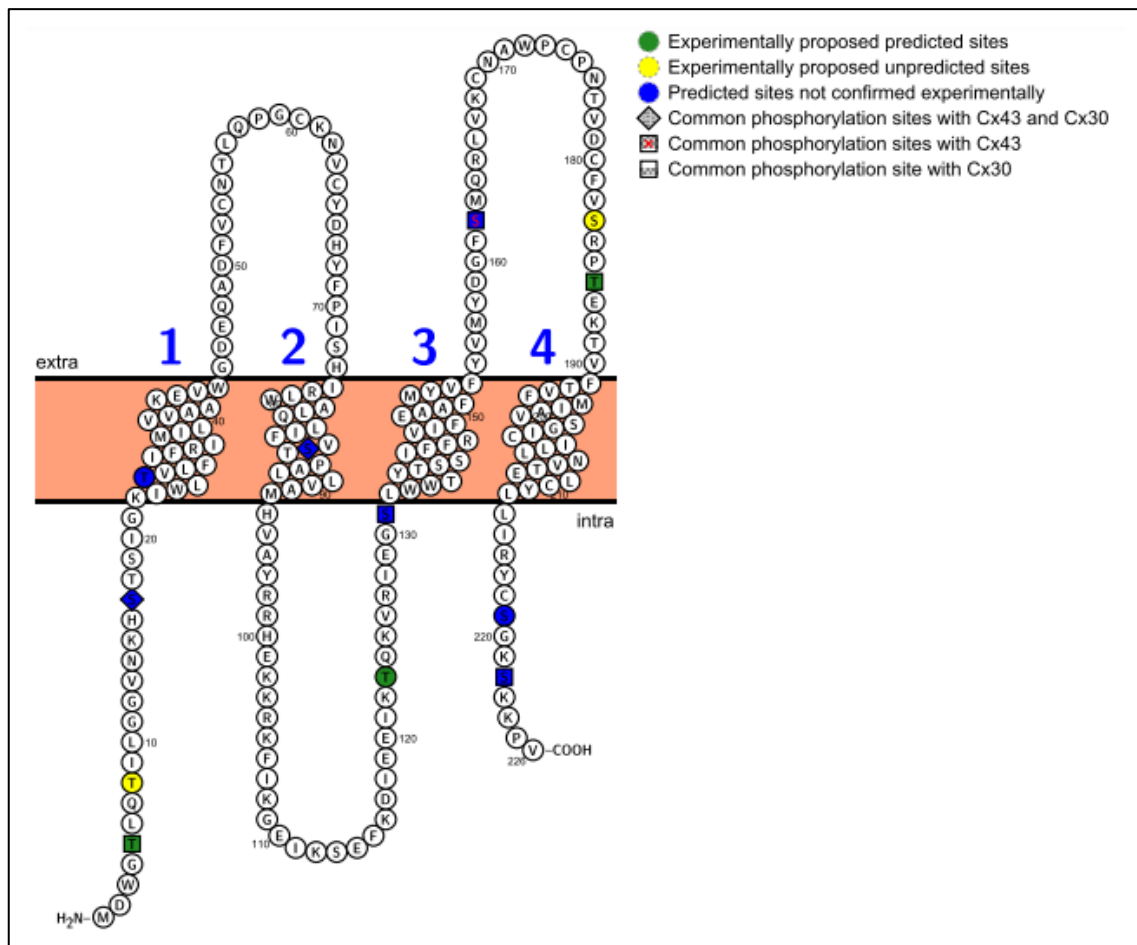


Figure 4.7: Cx26 topology and phosphorylation sites visualization by Protter.

4.3 Connexin 30 topology

We notice that Cx30 C-terminal domain is small (45 amino acids) but still bigger than its N-terminal domain (21 amino acids).

Thirteen phosphorylation sites were predicted for Cx30, experimentally confirmed sites are shown in green, and the non-confirmed are shown in blue. The latter eight were predicted for the first time are S17 and T18 in the N-terminal region, S85 in the second extracellular domain, T103 and S131 in the cytoplasmic loop, T186 in the second extracellular loop, S199 in the fourth transmembrane domain and T227 in its C-terminal domain.

Cx30 shares two common phosphorylation sites with Cx43 and Cx26 which are S17 and S85 (represented in a diamond shape), it also shares four common sites with Cx26 (represented in a square shape) which are T5, S131, T186 and S222 (**Figure 4.8**).

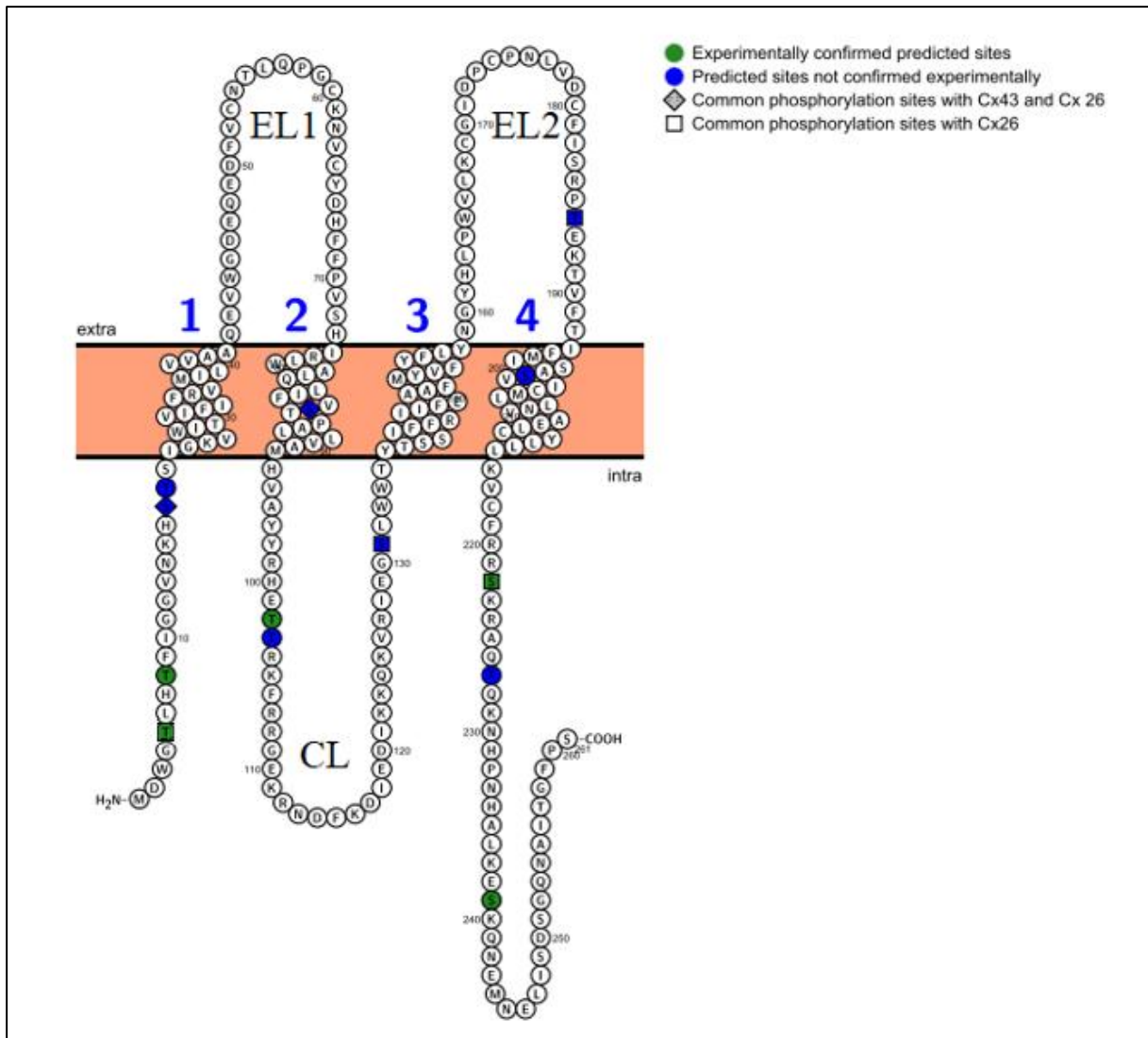


Figure 4.8: Cx30 topology and phosphorylation sites visualization by Protter.

Connexin phosphorylation through several protein kinases have multiple roles in the formation and regulation of Gap junction channels and hemichannels including oligomerization, trafficking, protein-protein interaction and channel gating (Pogoda *et al.*, 2016). p38 α response to physio-pathological conditions generated by reactive oxygen species or inflammatory cytokines (Canovas and Nebreda, 2021). Thus, it may be possible that lower pH, mechanical stimulation, oxidative stress and inflammation observed in neurodegenerative diseases can activate signaling pathways involving specific kinases, leading to the phosphorylation at specific sites of connexins therefore dysregulating GJC and HC activity. For that we explored *in silico* the potential phosphorylation sites of astrocytic connexins.

The three connexins, one of the α group Cx43 and two of the β group Cx26 and Cx30 are expressed in astrocytes (Sanchez *et al.*, 2020, Huang *et al.*, 2021), our results show that these proteins are phosphoproteins which is consistent with the results of Locke *et al.* (2009), Alstrøm

et al. (2015) and Leithe *et al.* (2018). In the literature, very few studies have been carried out on Cx26 and Cx30 phosphorylation, thus only a few sites have been proposed or confirmed (Locke *et al.*, 2009; Alstrøm *et al.*, 2015) unlike Cx43 which has been heavily studied. Several research confirmed the effects of different kinases on multiple sites in its carboxy-terminal domain causing conformational changes of the connexin and then modulating gap junction intercellular channel and also hemichannel gating (Pogoda *et al.*, 2016; Leithe *et al.*, 2018, Sanchez *et al.*, 2020). While Cx43 presents confirmed phosphorylation sites only in its carboxy-terminal end, Cx26 and Cx30 present confirmed or potential sites at multiple domains of the proteins. In our research, Netphos 3.1 predicted phosphorylation sites in all three connexins at different localizations, which showed a predominance at the carboxy-terminal domain for Cx43. Interestingly, our work managed to predict three new noteworthy sites in Cx43 that could interfere with the cytoplasmic loop-carboxy-terminal interaction described by Iyathurrai *et al.* (2017). These sites are S273, Y286 and T290, since they are adjacent to domains responsible for the interaction described by the previously mentioned study, their phosphorylation may be involved with the regulation of the junctional channels and/or hemichannels permeability. The cytoplasmic loop-carboxy-terminal interaction is also confirmed for Cx26 even with its short C-terminus (Locke *et al.*; 2011). It is possible that our newly predicted phosphorylation sites of Cx26, which are S219 and S222 in the carboxy-terminal domain and S131 in the cytoplasmic loop domain, play a role in the CL-CT interaction. The second connexin of the β group Cx30 presents also newly predicted phosphorylation sites which are T103 and S131 in its cytoplasmic loop, and T227 in its carboxy terminal end, suggesting that these sites also may play a role in this interaction.

As Cx43, Cx26 and Cx30 are the three astrocyte connexins, it seemed right to analyze their common predicted phosphorylation sites. The analysis points to the following, Cx43, Cx26 and Cx30 share the S17 (S18 for Cx43) in their amino-terminal ends, that may have no significant function since it is far from the voltage sensing amino acids described in the review of Leybaert *et al.* (2017). They also share the strange site in the second transmembrane domain S85 (S86 for Cx43), as phosphorylation in the transmembrane domain is not explored. Interestingly, both Cx26 and Cx30 share the S5 predicted site as an experimentally confirmed phosphorylation site, which is responsible for the formation of NT plug described for Cx26 by Oshima (2014), thus its phosphorylation can alter the plug formation. Cx26 and Cx30 share the newly predicted site S131 in the cytosolic loop, which neighbors the WW-motif. This motif is responsible for heterotypic compatibility of connexons. This may suggest that the phosphorylation of this site may interfere with the function of the WW-motif (Aasen *et al.*, 2018). Cx26 and Cx30 also

share the predicted site T186 in the second extracellular domain, and S222 in the carboxy-terminal end. It was also predicted that Cx26 shares a phosphorylation site with Cx43 in the second extracellular domain S162 (180 for Cx43).

Conclusion

In this work, we were interested in the study of astrocytic connexins (Cx43, Cx26 and Cx30), recognizing their crucial role in the intricate mechanisms of brain function. Astrocytes, through connexin-mediated gap junctions, facilitate intercellular communication essential for maintaining homeostasis and supporting neuronal activity. Recent studies have increasingly implicated connexins in the pathophysiology of neurodegenerative diseases. These diseases can lead to the phosphorylation of specific sites of connexins therefore dysregulating gap junction channels and hemichannels activity. This suggests that these proteins may be potential therapeutic targets.

In this study, we focused on astrocytic connexins using an *in silico* approach. The topology analysis with ΔG predictor allowed us to characterize the four transmembrane domains for Cx43, Cx26 and Cx30. Concerning the prediction of phosphorylation sites, our research confirmed that Cx43 phosphorylation sites cluster in its carboxy-terminal end unlike Cx26 and Cx30. Their phosphorylation sites are rather localized, in N-terminal region, second transmembrane segment as well as cytosolic loop, second extracellular loop and C-terminal domains.

Our work revealed multiple phosphorylation sites for the first time. The most interesting sites predicted are sites that could interfere with the regulating cytoplasmic loop-carboxy-terminal interaction which are S273, Y286 and T290 in the carboxy-terminal end for Cx43. The sites S219 and S222 in the carboxy-terminal end and S131 in the cytoplasmic loop domain for Cx26. The sites T103 and S131 in the cytoplasmic loop, and T227 in the carboxy terminal end for Cx30.

Finally, the comparative alignment of the three connexins uncovered features either shared between all three connexins or in pairs. Cx43, Cx26 and Cx30 shared the sites S17 (S18 for Cx43) in the N-terminal and S85 (S86 for Cx43) in the second transmembrane domain. We couldn't allocate a clear involvement in connexin regulation for these sites. Furthermore, Cx26 and Cx43 shared S162 (S180 for Cx43) which is localized in the second extracellular loop.

Finally, sites shared between Cx26 and Cx30 are S5 in the amino-terminal which may influence the formation of the N-terminal plug. The site S131 which is located in the cytoplasmic loop. S131 site neighbors the WW-motif who is responsible for heterotypic compatibility of connexons. The site T186 in the second extracellular loop is also shared. The site S222 located in the carboxy-terminal end may be involved in the cytosolic loop-carboxy-terminal interaction. These first-time predicted sites could have a role in dysregulating astrocytic gap junction channels and hemichannels, during astrogliosis of neurodegenerative diseases.

In perspective, these results open the horizon to initiate other studies such as:

- Experimentally confirm the predicted sites.
- Experimentally pinpointing the kinases and their activation pathways responsible for the phosphorylation of astrocytic connexins.
- *In silico* study of other post-translational modifications for astrocytic connexins, and their roles in modulating gap junction channels and hemichannels.

References

-A-

Aasen, T., Johnstone, S., Vidal-Brime, L., Lynn, K. S., & Koval, M. (2018). Connexins: Synthesis, post-translational modifications, and trafficking in health and disease. *International journal of molecular sciences*, *19*(5), 1296.

Alberts, B. (2015) *Molecular Biology of the Cell*. 6th Edition, Garland Science, Taylor and Francis Group, New York.

Allen, N. J., & Barres, B. A. (2009). Glia—more than just brain glue. *Nature*, *457*(7230), 675-677.

Alstrøm, J. S., Hansen, D. B., Nielsen, M. S., & MacAulay, N. (2015). Isoform-specific phosphorylation-dependent regulation of connexin hemichannels. *Journal of Neurophysiology*, *114*(5), 3014-3022.

Axelsen, L. N., Calloe, K., Holstein-Rathlou, N. H., & Nielsen, M. S. (2013). Managing the complexity of communication: regulation of gap junctions by post-translational modification. *Frontiers in pharmacology*, *4*, 130.

-B-

Bargiello, T. A., Oh, S., Tang, Q., Bargiello, N. K., Dowd, T. L., & Kwon, T. (2018). Gating of Connexin Channels by transjunctional-voltage: Conformations and models of open and closed states. *Biochimica et Biophysica Acta (BBA)-Biomembranes*, *1860*(1), 22-39.

Beyer, E. C., Paul, D. L., & Goodenough, D. A. (1987). Connexin43: a protein from rat heart homologous to a gap junction protein from liver. *The Journal of cell biology*, *105*(6), 2621-2629.

Blom, N., Sicheritz-Pontén, T., Gupta, R., Gammeltoft, S., & Brunak, S. (2004). Prediction of post-translational glycosylation and phosphorylation of proteins from the amino acid sequence. *Proteomics*, *4*(6), 1633-1649.

Bukauskas, F. F., & Verselis, V. K. (2004). Gap junction channel gating. *Biochimica et Biophysica Acta (BBA)-Biomembranes*, *1662*(1-2), 42-60.

-C-

Canovas, B., & Nebreda, A. R. (2021). Diversity and versatility of p38 kinase signalling in health and disease. *Nature reviews Molecular cell biology*, *22*(5), 346-366.

Chever, O., Lee, C. Y., & Rouach, N. (2014). Astroglial connexin43 hemichannels tune basal excitatory synaptic transmission. *Journal of Neuroscience*, *34*(34), 11228-11232.

-D-

De Vuyst, E., Wang, N., Decrock, E., De Bock, M., Vinken, M., Van Moorhem, M., ... & Leybaert, L. (2009). Ca²⁺ regulation of connexin 43 hemichannels in C6 glioma and glial cells. *Cell calcium*, 46(3), 176-187.

-G-

Giaume, C., Koulakoff, A., Roux, L., Holcman, D., & Rouach, N. (2010). Astroglial networks: a step further in neuroglial and gliovascular interactions. *Nature Reviews Neuroscience*, 11(2), 87-99.

Goodenough, D. A., & Paul, D. L. (2009). Gap junctions. *Cold Spring Harbor Perspectives in Biology*, 1(1), a002576.

Goodenough, D. A., Goliger, J. A., & Paul, D. L. (1996). Connexins, connexons, and intercellular communication. *Annual review of biochemistry*, 65(1), 475-502.

-H-

Hessa, T., Kim, H., Bihlmaier, K., Lundin, C., Boekel, J., Andersson, H., ... & von Heijne, G. (2005). Recognition of transmembrane helices by the endoplasmic reticulum translocon. *Nature*, 433(7024), 377-381.

Hessa, T., Meindl-Beinker, N. M., Bernsel, A., Kim, H., Sato, Y., Lerch-Bader, M., ... & Von Heijne, G. (2007). Molecular code for transmembrane-helix recognition by the Sec61 translocon. *Nature*, 450(7172), 1026-1030.

Huang, X., Su, Y., Wang, N., Li, H., Li, Z., Yin, G., ... & Yi, C. (2021). Astroglial connexins in neurodegenerative diseases. *Frontiers in molecular neuroscience*, 14, 657514.

-I-

Iyyathurai, J., Wang, N., D'hondt, C., Jiang, J. X., Leybaert, L., & Bultynck, G. (2018). The SH3-binding domain of Cx43 participates in loop/tail interactions critical for Cx43-hemichannel activity. *Cellular and molecular life sciences*, 75, 2059-2073.

-K-

Kinnamon, S. C., & Finger, T. E. (2013). A taste for ATP: neurotransmission in taste buds. *Frontiers in cellular neuroscience*, 7, 264.

Kirichenko, E. Y., Skatchkov, S. N., & Ermakov, A. M. (2021). Structure and functions of gap junctions and their constituent connexins in the mammalian CNS. *Biochemistry (Moscow), Supplement Series A: Membrane and Cell Biology*, 15(2), 107-119.

Koulakoff, A., Mei, X., Orellana, J. A., Sáez, J. C., & Giaume, C. (2012). Glial connexin expression and function in the context of Alzheimer's disease. *Biochimica et Biophysica Acta (BBA)-Biomembranes*, 1818(8), 2048-2057.

-L-

Leybaert, L., Lampe, P. D., Dhein, S., Kwak, B. R., Ferdinandy, P., Beyer, E. C., ... & Schulz, R. (2017). Connexins in cardiovascular and neurovascular health and disease: pharmacological implications. *Pharmacological reviews*, 69(4), 396-478.

Li, C., Meng, Q., Yu, X., Jing, X., Xu, P., & Luo, D. (2012). Regulatory effect of connexin 43 on basal Ca²⁺ signaling in rat ventricular myocytes. *PloS one*, 7(4), e36165.

Locke, D., Bian, S., Li, H., & Harris, A. L. (2009). Post-translational modifications of connexin26 revealed by mass spectrometry. *Biochemical Journal*, 424(3), 385-398.

Locke, D., Kieken, F., Tao, L., Sorgen, P. L., & Harris, A. L. (2011). Mechanism for modulation of gating of connexin26-containing channels by taurine. *Journal of General Physiology*, 138(3), 321-339.

Locke, D., Koreen, I. V., Harris, A. L., Locke, D., Koreen, I. V., & Harris, A. L. (2006). Isoelectric points and post-translational modifications of connexin26 and connexin32. *The FASEB journal*, 20(8), 1221-1223.

-M-

Madeira, F., Madhusoodanan, N., Lee, J., Eusebi, A., Niewielska, A., Tivey, A. R., ... & Butcher, S. (2024). The EMBL-EBI Job Dispatcher sequence analysis tools framework in 2024. *Nucleic Acids Research*, gkae241.

Maes, M., Decrock, E., Cogliati, B., Oliveira, A. G., Marques, P. E., Dagli, M. L., ... & Vinken, M. (2014). Connexin and pannexin (hemi) channels in the liver. *Frontiers in physiology*, 4, 405.

Mayorquin, L. C., Rodriguez, A. V., Sutachan, J. J., & Albarracín, S. L. (2018). Connexin-mediated functional and metabolic coupling between astrocytes and neurons. *Frontiers in molecular neuroscience*, 11, 118.

-O-

Omasits, U., Ahrens, C. H., Müller, S., & Wollscheid, B. (2014). Protter: interactive protein feature visualization and integration with experimental proteomic data. *Bioinformatics*, 30(6), 884-886.

Orellana, J. A., Froger, N., Ezan, P., Jiang, J. X., Bennett, M. V., Naus, C. C., ... & Sáez, J. C. (2011). ATP and glutamate released via astroglial connexin 43 hemichannels mediate neuronal death through activation of pannexin 1 hemichannels. *Journal of neurochemistry*, 118(5), 826-840.

Orellana, J. A., Sáez, P. J., Shoji, K. F., Schalper, K. A., Palacios-Prado, N., Velarde, V., ... & Sáez, J. C. (2009). Modulation of brain hemichannels and gap junction channels by pro-

inflammatory agents and their possible role in neurodegeneration. *Antioxidants & redox signaling*, 11(2), 369-399.

Oviedo-Orta, E., & Evans, W. H. (2004). Gap junctions and connexin-mediated communication in the immune system. *Biochimica et Biophysica Acta (BBA)-Biomembranes*, 1662(1-2), 102-112.

-P-

Peracchia, C. (2004). Chemical gating of gap junction channels: roles of calcium, pH and calmodulin. *Biochimica et Biophysica Acta (BBA)-Biomembranes*, 1662(1-2), 61-80.

Pogoda, K., Kameritsch, P., Retamal, M. A., & Vega, J. L. (2016). Regulation of gap junction channels and hemichannels by phosphorylation and redox changes: a revision. *BMC cell biology*, 17, 137-150.

Purves, D., Augustine, G. J., Fitzpatrick, D., Hall, W. C., LaMantia, A.-S., McNamara, J. O., & Williams, S. M. (Eds.). (2004). *Neuroscience* (3rd ed.). Sinauer Associates.

-R-

Rash, J. E., Yasumura, T., Davidson, K. G. V., Furman, C. S., Dudek, F. E., & Nagy, J. (2001). Identification of cells expressing Cx43, Cx30, Cx26, Cx32 and Cx36 in gap junctions of rat brain and spinal cord. *Cell communication & adhesion*, 8(4-6), 315-320.

Retamal, M. A., Alcayaga, J., Verdugo, C. A., Bultynck, G., Leybaert, L., Sáez, P. J., ... & Sáez, J. C. (2014). Opening of pannexin-and connexin-based channels increases the excitability of nodose ganglion sensory neurons. *Frontiers in cellular neuroscience*, 8, 158.

Retamal, M. A., Cortés, C. J., Reuss, L., Bennett, M. V., & Sáez, J. C. (2006). S-nitrosylation and permeation through connexin 43 hemichannels in astrocytes: induction by oxidant stress and reversal by reducing agents. *Proceedings of the National Academy of Sciences*, 103(12), 4475-4480.

Retamal, M. A., Reyes, E. P., García, I. E., Pinto, B., Martínez, A. D., & González, C. (2015). Diseases associated with leaky hemichannels. *Frontiers in cellular neuroscience*, 9, 267.

-S-

Sáez, J. C., Berthoud, V. M., Branes, M. C., Martínez, A. D., & Beyer, E. C. (2003). Plasma membrane channels formed by connexins: their regulation and functions. *Physiological reviews*, 83(4), 1359-1400.

Saidi Brikci-Nigassa, A. (2015). *Domaine juxta-membranaire de la connexine43 : Détermination par RMN en solution de la structure et de l'interaction avec la tubuline et les microtubules* [Doctoral dissertation, Abou Bekr Belkaid University Tlemcen]. Depot

institutionnel de l'Université Abou Bekr Belkaid Tlemcen UABT. <http://dspace1.univ-tlemcen.dz/handle/112/7217>

Sánchez, O. F., Rodríguez, A. V., Velasco-España, J. M., Murillo, L. C., Sutachan, J. J., & Albarracín, S. L. (2020). Role of connexins 30, 36, and 43 in brain tumors, neurodegenerative diseases, and neuroprotection. *Cells*, 9(4), 846.

Stehberg, J., Orellana Roca, J. A., & Sáez, J. C. (2012). Release of gliotransmitters through astroglial connexin 43 hemichannels is necessary for fear memory consolidation in the basolateral amygdala.

-T-

Traub, O., Look, J., Dermietzel, R., Brümmer, F., Hülser, D., & Willecke, K. (1989). Comparative characterization of the 21-kD and 26-kD gap junction proteins in murine liver and cultured hepatocytes. *The Journal of cell biology*, 108(3), 1039-1051.

-V-

Vinken, M., Decrock, E., De Vuyst, E., Ponsaerts, R., D'hondt, C., Bultynck, G., ... & Rogiers, V. (2011). Connexins: sensors and regulators of cell cycling. *Biochimica et Biophysica Acta (BBA)-Reviews on Cancer*, 1815(1), 13-25.

-W-

Waterhouse, A. M., Procter, J. B., Martin, D. M., Clamp, M., & Barton, G. J. (2009). Jalview Version 2—a multiple sequence alignment editor and analysis workbench. *Bioinformatics*, 25(9), 1189-1191.

Willecke, K., Eiberger, J., Degen, J., Eckardt, D., Romualdi, A., Güldenagel, M., ... & Söhl, G. (2002). Structural and functional diversity of connexin genes in the mouse and human genome.

Willecke, K., Eiberger, J., Degen, J., Eckardt, D., Romualdi, A., Güldenagel, M., ... & Söhl, G. (2002). Structural and functional diversity of connexin genes in the mouse and human genome.

-Z-

Zhang, M., Wang, Z. Z., & Chen, N. H. (2023). Connexin 43 Phosphorylation: Implications in Multiple Diseases. *Molecules*, 28(13), 4914.